

DISSERTATION

COMPARISON OF RADIOBIOLOGICAL ENDPOINTS IN CELLS
FROM CXB RI MICE

Submitted by

Guanxiong Xiao

Graduate Degree Program in Cell and Molecular Biology

In partial fulfillment of the requirements

For the Degree of Doctor of Philosophy

Colorado State University

Fort Collins, Colorado

Spring 2008

UMI Number: 3321323

INFORMATION TO USERS

The quality of this reproduction is dependent upon the quality of the copy submitted. Broken or indistinct print, colored or poor quality illustrations and photographs, print bleed-through, substandard margins, and improper alignment can adversely affect reproduction.

In the unlikely event that the author did not send a complete manuscript and there are missing pages, these will be noted. Also, if unauthorized copyright material had to be removed, a note will indicate the deletion.

UMI[®]

UMI Microform 3321323

Copyright 2008 by ProQuest LLC.

All rights reserved. This microform edition is protected against unauthorized copying under Title 17, United States Code.

ProQuest LLC
789 E. Eisenhower Parkway
PO Box 1346
Ann Arbor, MI 48106-1346

COLORADO STATE UNIVERSITY

April 1, 2008

WE HEREBY RECOMMEND THAT THE DISSERTATION PREPARED UNDER OUR SUPERVISION BY GUANXIONG XIAO ENTITLED "COMPARISON OF RADIOBIOLOGICAL ENDPOINTS IN CELLS FROM CXB RI MICE" BE ACCEPTED AS FULFILLING IN PART REQUIREMENTS FOR THE DEGREE OF DOCTOR OF PHILOSOPHY.

Committee on Graduate Work



Joel S. Bedford



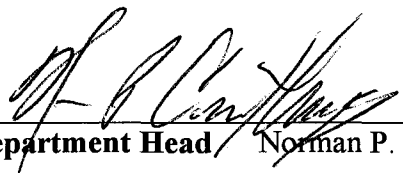
Robert L. Ullrich



Ann M. Hess



Adviser Michael M. Weil



Department Head Norman P. Curthoys

ABSTRACT OF DISSERTATION

COMPARISON OF RADIOBIOLOGICAL ENDPOINTS IN CELLS FROM CXB RI MICE

Recombinant inbred (RI) mouse strains have been used both for trait cosegregation studies and genetic linkage analysis. They are created by using a breeding scheme that consists of a cross between two inbred mouse strains (progenitor strains) followed by at least 20 generations of brother-sister inbreeding. Thus, RI strains are inbred (homozygous at every locus) and derive roughly half their genome from each of the two progenitor strains. The CXB RI strain set consists of 13 RI strains derived from matings of BALB/c (C) and C57BL/6(B) mice.

The CXB progenitor strains, BALB/c and C57BL/6, differ in their susceptibility to radiation-induced mammary tumors with BALB/c being susceptible and C57BL/6 being resistant. In part, the susceptibility difference can be explained by a polymorphism in the *Prkdc* gene which encodes the catalytic subunit of DNA-dependent protein kinase. However, other, as yet unknown, loci may be involved. The CXB RI strain set provides a useful tool to unravel the events that lead to radiation-induced mammary tumorigenesis and to understand the interrelationships of cellular radiobiological endpoints to one-another.

We have generated fibroblast strains from each of the CXB RI strains and from the progenitor strains. The fibroblast strains were assayed for a number of radiobiological endpoints including clonogenic survival following acute and low dose-rate exposures, γ -H2AX focus formation and clearance following acute and low dose-rate exposures, and G2 chromosomal aberrations. In addition, we genotyped the strains for a polymorphism in the gene encoding the catalytic subunit of the DNA-dependent protein kinase, *Prkdc*. We then determined the correlations of different endpoints between the RI strains. As expected, clonogenic survival at low dose rates and following acute exposures were positively correlated. γ -H2AX focus formation at low dose rate correlated well with survival endpoints, particularly clonogenic survival under low dose rate irradiation and the surviving fraction at 2 Gy acute exposures. These three endpoints are all significantly associated with the *Prkdc* genotype with radiosensitive strains having the BALB/c genotype.

The data we have collected provides a baseline description of cellular radiosensitivity in CXB fibroblasts. The approach used in this dissertation can be used to correlate these cellular radiobiological endpoints with susceptibility to clinically significant adverse outcomes from cancer radiotherapy, such as normal tissue injury and radiation-induced second cancers.

Guanxiong Xiao
Graduate Degree Program in Cell and Molecular Biology
Colorado State University
Fort Collins, Colorado 80523
Spring 2008

Table of Content

Introduction	page
Introduction.....	1
Ionizing Radiation and DNA double stand breaks.....	2
DNA damage response after DSB.....	4
DNA-PK.....	11
Ataxia-Telangiectasia.....	13
Assays of cellular radiosensitivity.....	20
γ -H2AX.....	23
G2 Chromosomal Radiosensitivity.....	27
Recombinant Inbred Mice.....	28
Correlating Traits in Genetically Randomized Populations.....	30
Materials and Methods	
Cell culture.....	31
Acute dose irradiation.....	32
Low Dose Rate Irradiation.....	33
γ -H2AX Analysis Following Acute Exposure.....	34
γ -H2AX formation under low dose-rate.....	36
G2 Chromosome Analysis.....	38
Genotyping.....	40
Results	
<i>Prkdc</i> Genotyping.....	41
Clonogenic Survival.....	41

SF2.....	42
Survival at Low Dose Rate.....	42
Acute dose γ -H2AX Focus formation.....	43
Low dose rate γ -H2AX Foci.....	44
Tables of results.....	49
Figures of results.....	55
Discussion	83
Reference	90

ACKNOWLEDGEMENT

I would first like to extend my appreciation to all the people who were involved in my admission to CSU. Without them, I could not have come to this beautiful state, become a member of such a great group, have met so many nice and intelligent people, and furthermore, I could not have experienced these 6 most important and also most incredible years in my life.

My advisor, Dr. Michael Weil, was a great inspiration to my work and I truly appreciated his assistance throughout my entire graduate student life. From him, I learned science and research as well as respect and generosity. His brilliant research ideas and moral support in the lab always helped me out of any dilemmas. And I thank Dr. Nagasawa for sharing her experiences in tissue culture and survival curve analysis. She helped me on every experiment in my project, and talking to her has always been inspiring and helpful.

My committee members, Dr. Joel Bedford, Dr. Robert Ullrich, and Dr. Ann Hess were always providing assistance when I was in need. I wish to extend my thanks to my colleagues. Dr. Paula Genik, Dr. Yuanlin Peng, Dr. Xian'an Liu provided great discussion and excellent advices. Alexander Roby helped me to on G2 chromosome aberration analysis.

Finally, a special thanks to my family and all of my friends, for their unconditional support and listening to me when I was stressed. For this I will be eternally grateful.

Introduction

A number of different radiobiological endpoints have been used to quantify radiosensitivity in cells. Among these are assays for clonogenic survival, cell cycle delay, apoptosis, DNA rejoining, γ -H2AX focus formation and resolution, and chromosome aberrations. Interindividual differences in sensitivity as measured by these endpoints is a common feature of the assays and for radiation-induced apoptosis differences between mouse strains have also been described. In some cases, attempts have been made to correlate cellular radiosensitivity with clinically relevant conditions, specifically cancer susceptibility and normal tissue injury from radiotherapy. The prototype and most striking example for association of a cellular radiosensitivity with a clinical phenotype is ataxia-telangiectasia (A-T). Here, we provide background on how cells repair DNA damage from ionizing radiation, review radiosensitivity in A-T and describe some of the assays available to quantify cellular radiosensitivity. We then describe an approach using recombinant inbred (RI) strains of mice to correlate cellular measures of radiosensitivity with one another, with genetic polymorphisms suspected of determining radiosensitivity, and with clinically relevant phenotypes. Finally, as proof of principle, we present results we have generated comparing assays of cellular radiosensitivity in the CXB recombinant inbred mouse panel.

Ionizing Radiation and DNA double stand breaks

Some radiation has enough energy to eject one or more orbital electrons from an atom or molecule; this radiation is called ionizing radiation (IR). IR always causes large amount energy release, and this energy is more than enough to break some strong chemical bonds. In biologic research, x- or γ - rays are used a lot as ionizing radiation sources. X- and γ - are two forms of electromagnetic radiation and they do not differ in nature. They differ in the ways they are produced: γ -rays are produced within the nucleus and x-rays are produced extranuclearly. There are some other types of radiations in nature, like electrons, protons, α -particles, neutrons and heavy charged ions. These are also used experimentally in biological research. These charged particles are directly ionizing, because they are individual particles with sufficient kinetic energy. They can directly disrupt the atomic structure of the target they traverse. Electromagnetic radiations (x- and γ - rays) are indirectly ionizing, because they do not produce chemical and biologic damage themselves. However, after they are absorbed by biologic target, they will give up their energy and produce fast moving charged particles. These particles can cause chemical and biologic damage in target materials.

When biologic materials absorb radiation, damage can occur in two ways. If a biological molecule is directly ionized, then a biologic change on this target may result from the interaction. This is called direct action of radiation. In another situation, radiation may not directly interact directly with target atoms but rather with other atoms or molecules (particularly water) to produce free radicals. These

free radicals can diffuse far enough to damage the biologic targets. This is called indirect action of radiation. A free radical is an atom or molecule carrying an unpaired orbital electron in the outer shell. In this state an atom or molecule is very unstable and has high degree of chemical reactivity.

Biologically, the most important damage caused by ionizing radiation in cells is DNA strand breaks. After the energy from IR is absorbed by biologic target, it can form 3 different energy events: spurs, blobs and short tracks. In the case of x- and γ -rays, 95% of the energy events are spurs, which have a diameter of about 4nm - about twice the diameter of the DNA double helix and contain up to 100eV energy. The diameter of a blob diameter is about 7nm and contains 100-500eV energy. Because these energy events (spur and blob) have dimensions similar to the DNA double helix (2nm), they can cause multiple radical attack resulting in DNA double strand breaks (DSBs) or single strand breaks (SSBs) when they overlap the DNA helix. Single strand breaks are the most common type of DNA damage caused by IR, but SSBs have little biologic consequence because they are readily repaired. If two SSBs occur on opposite DNA strands separated by only a few base pairs a double strand break may result. As described later, DSBs may cause severe problems in cells (Hall, E.J. *et al*, Radiobiology for the radiologist, sixth edition, 2006).

DNA damage response after DSB

There are many agents that can cause damage to the DNA in cells. These agents include ultraviolet light, man-made and natural occurring mutagenic chemicals, and reactive oxygen species generated by ionizing radiation (IR), or by processes such as redox cycling by heavy metal ions and radio-mimetic drugs (Friedberg *et al.* 1995; Hoeijmakers *et al.* 2001). They can cause many forms of damage; probably the most dangerous is the DNA double-strand break. DNA-damaging agents can break two complementary strands of the DNA double helix simultaneously. If these two breaks are close enough to one another, base-pairing and chromatin structure cannot keep the two DNA ends juxtaposed, then DNA DSBs are generated (Jackson, 2002). The dissociation of the two DNA ends caused by DSBs makes the repair difficult and these DNA ends may inappropriately recombine with other sites in the genome. DSBs can induce mutations through direct disruption of the DNA sequence or can induce cell death by apoptosis (Rich *et al.* 2000). These mutations generated by DSBs may have a link with tumorigenic potential (Lengauer, *et al.* 1998; Khanna, *et al.* 2001; Ferguson *et al.* 2001).

Cells have rapid and efficient systems to repair the damage caused by DNA DSBs. Some of these systems are signal-transduction cascades (Figure 1-1) that are set in motion by DNA-damage binding proteins that detect DNA damage and trigger protein kinase cascades. The relevant protein kinases include ATM, ATR,

DNA-PKcs, and others; we will discuss them later. Then, these protein kinases amplify and diversify the signal of DNA damage to generate a downstream DNA-damage response. In dividing cells DNA DSBs will slow down or stop the progression of cell cycle. For example, DNA damage generated in G1 or S phase can prevent the cell from entering S-phase, or slow its progression through S-phase. This system provides enough time for DNA to be repaired before it is replicated. Similarly, if DNA DSBs are generated in the G2-phase, the entry into mitosis is stopped. This will prevent the segregation of the damage during cytokinesis. All these cell-cycle pausing systems are termed 'cell-cycle checkpoints' (Zhou, *et al.* 2000; Bartek, *et al.* 2001). There are other non-cycle related DNA damage responses, like chromatin structure reorganization. In yeast, phosphorylation of histone H2A will lead to chromatin structure reorganization (Downs, *et al.* 2000); in mammals, this alternation is triggered by phosphorylation of the histone H2A iso-form, H2AX (γ -H2AX) (Rogakou, *et al.* 1998). The chromatin structure change at the site of DNA damage makes the damaged site more accessible to DNA repair complexes. If the DNA damage is too great to be repaired, the cell may enter an apoptotic program (Rich, *et al.* 2000; Hirao, *et al.* 2000; Herzog, *et al.* 1998).

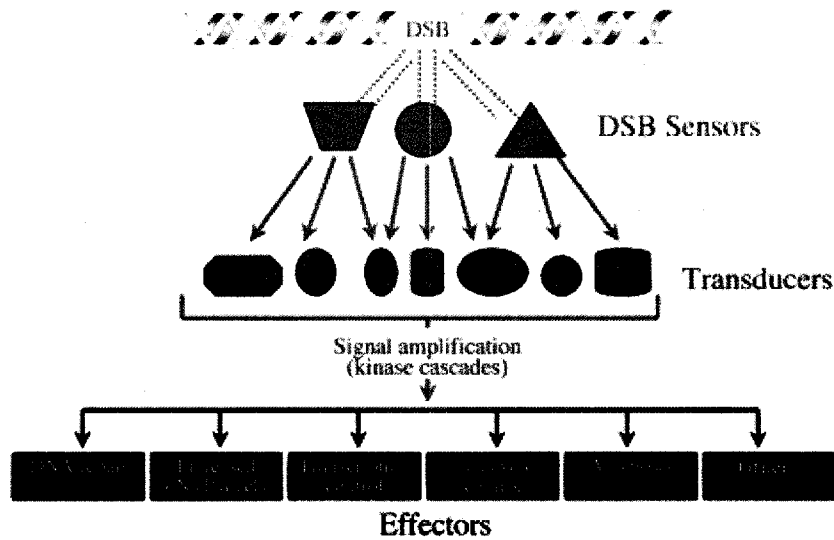


Figure 1-1 Cellular response to DNA DSBs. From *Sensing and repairing DNA double strand breaks*. Jackson SP, *Carcinogenesis* vol 23, no.5, pp. 687-696,

2002

There are two main DNA DSB repair pathways: homologous recombination (HR) and non-homologous end-joining (NHEJ). These pathways are different and function complementarily on DNA DSBs repair (Cromie, *et al.* 2001; Haber, *et al.* 2000; Takata, *et al.* 1998; Essers, *et al.* 2000). In simple eukaryotes, like yeasts, HR is the main pathway for DNA damage repair. In mammals, NHEJ plays an important role in G0 and G1, and HR is important in S- and G2-phase (Johnson, *et al.* 2000).

There are at least 4 steps in NHEJ pathway: (1) detection of a DSB; (2) formation of a molecular bridge that holds the DNA ends together; (3) a processing procedure that modifies non-matching and/or damaged DNA ends into compatible and ligatable ends; and (4) the final ligation (Weterings, *et al.*, 2004).

Several gene products are involved in these 4 steps–DNA-dependent protein kinase catalytic subunit (DNA-PKcs), Ku70/80 heterodimer, DNA ligase IV and XRCC4. DNA-PKcs is a 469kDa catalytic subunit of DNA-PK holo-enzyme (DNA-PK) that also includes the Ku70/80 dimer (Smith, *et al* 1999; Lees-Miller, *et al* 2003). DNA-PKcs has serine/threonine protein kinase activity, and this activity is enhanced by association with Ku70/80 and DNA. The Ku70/80 heterodimer can form a hollow ring around the DNA helix to bind to DNA; Ku70 and Ku80 each making up half of the ring (Walker, *et al* 2001). This structure gives the Ku70/80 heterodimer high affinity for DNA, and the Ku ring can slide on the DNA (Smith, *et al* 1999). The Ku70/80 dimer attracts DNA-PKcs after it binds to DNA ends. Although DNA-PKcs can bind to DNA ends by itself, it dissociates very easily from the DNA helix. The binding of both Ku and DNA-PKcs to DNA ends activates the serine/threonine kinase activity of DNA-PKcs. This kinase activity is very important in NHEJ pathway; DNA-PKcs can function in a signal transduction cascade by phosphorylating TP53, XRCC4, Ku and itself (auto-phosphorylation) (Lakin, *et al* 1999). Ligation of DNA DSB ends in NHEJ pathway is accomplished by the DNA ligase IV/XRCC4 complex. After phosphorylation by DNA-PKcs, two XRCC4 molecules combine with one ligase IV molecule. This combination stabilizes and activates ligase IV in the NHEJ pathway. Then, the DNA DSB is reconnected by ligase IV.

Non-homologous end-joining

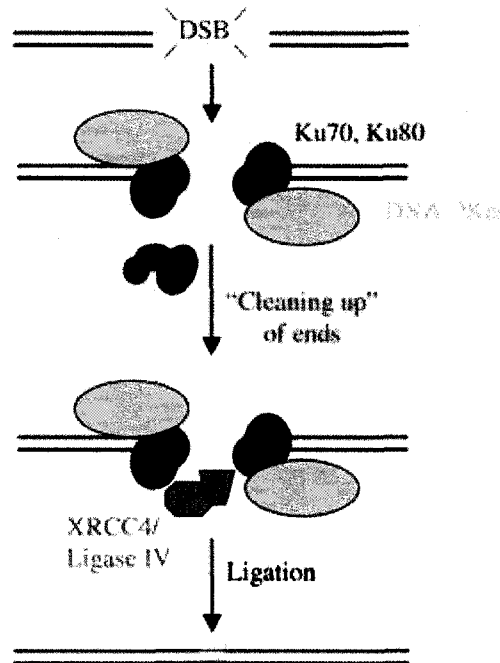


Figure 1-2 NHEJ repair pathway. From *Doherty AJ and Jackson SP. (2001) How Ku makes ends meet. Curr. Biol. 11:R920-R924*

The homologous recombination (HR) pathway of DNA repair was first defined by studies in bacteria and yeast, and this pathway is conserved in higher organisms. Several *S. cerevisiae* genes, *RAD50*, *RAD51*, *RAD52*, *RAD54*, *RAD55*, *RAD57*, *RAD59*, *MRE11* and *XRS2*, and their products play important roles in HR. Defects in these genes lead to increased sensitivity to ionizing radiation in *S. cerevisiae*. In mammals, the HR pathway is more complex, and more “RAD50 group” genes are involved (Wood, *et al.* 2001). The start of HR pathway *in vivo* depends on a complex containing RAD50, MRE11 and NBS1 (MRN complex). At the damage site on DNA, the 3' single strand tail is bound by RAD51 with the help of other proteins like replication protein A (RPA), RAD52 and RAD54.

RAD52 can compete with Ku for DNA ends, and this may determine which DSB repair pathway, NHEJ or HR, will be used (Van Dyck, *et al.* 1999). The nucleoprotein filament of RAD51 will interact with damaged DNA and look for the homologous region in a sister chromatid of homologous chromosome. After this region is located, the damaged DNA will invade into the undamaged DNA helix under the control of RAD51, to form a D-loop. In these events, other factors like RPA will play important roles (Petukhova *et al.* 1998). The 3' end of the damaged DNA copies information from the undamaged DNA and extends by a DNA polymerase; then DNA ligase I ligates the ends of the repaired DNA. Finally, DNA crossovers are cleaved and re-ligated to form two intact DNA molecules. Compared to NHEJ, the HR pathway is accurate and non-mutagenic; however, it takes much longer than NHEJ.

There are several other proteins involved in HR pathway, for example, RAD51B, RAD51C, RAD51D, XRCC2 and XRCC3. Some of these factors interact directly with RAD51 and help it to find the appropriate recombination substrate (Johnson, *et al.* 1999; Pierce, *et al.* 1999; Takata, *et al.* 2001; Liu, *et al.* 1998). Breast cancer susceptibility genes, BRCA1 and BRCA2 also involved in HR pathway. BRCA2 interact with RAD51 through its BRC motifs, so BRCA2 can affect both the nuclear location and DNA binding properties of RAD51 (Chen, *et al.* 1998; Davies, *et al.* 2001). BRCA1 can affect HR pathway by changing chromatin structure at the site of the DNA DSB.

Loss of important proteins in the HR pathway can lead to very serious problems

in cells. Inactivation of the *RAD51* will cause inviability of vertebrate tissue culture cells and early embryonic lethality in the mouse (Tsuzuki, *et al.* 1996; Sharan, *et al.* 1997; Sonoda, *et al.* 1998; Lim, *et al.* 1996). Disruption of *MRE11*, *RAD50* and/or *NBS1* will lead to same problems.

ATM also can affect HR pathway at DNA DSBs and as demonstrated in the chicken DT40 system (Morrison, *et al.* 2000). This effect may depend on the phosphorylation of the NBS1 and/or MRE11 by ATM at DNA DSBs (Lim, *et al.* 2000; Gatei, *et al.* 2000; Zhao, *et al.* 2000; Wu, *et al.* 2000). In addition, ATM can phosphorylate histone H2AX thus changing the chromatin structure at the sites of DNA DSBs; this also can affect HR pathway for DNA DSBs repair.

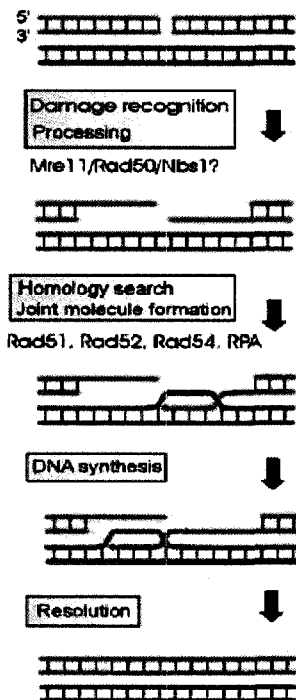


Figure 1.3 HR repair pathway. From *Eric Weterings and Dik C. van Gent, The mechanism of non-homologous end-joining: a synopsis of synapsis, DNA Repair 3 (2004) 1425–1435*

DNA-PK

DNA-PKcs is a nuclear serine/threonine kinase encoded by the *Prkdc* gene. The *Prkdc* gene was first discovered as a candidate gene responsible for the murine SCID phenotype (severe combined immunodeficient) (Kirchgessner, *et al.* 1995). The human *Prkdc* gene maps to 8q 11 and it encompasses a 12,228- bp open reading frame that encodes a 4127 amino acids poly-peptide with a molecular mass of ~470kDa. The gene has 86 exons (Siple, *et al.* 1995; ladenburger, *et al.* 1997). The DNA-PK holoenzyme is comprised of a regulatory subunit which contains Ku70/80, and a catalytic subunit, DNA-PKcs (Jeggo, *et al.*, 1995; Smith, *et al.*, 1999). Ku70 and Ku80 form a nonspecific DNA-binding heterodimer, and they exist in organisms ranging from yeast to man (Dyan, *et al.* 1998). DNA-PKcs, however, just exists in higher eukaryotes like human, mouse, horse and *Xenopus laevis*. A DNA-PKcs homolog has not been identified in the genome of *Saccharomyces cerevisiae* or *Caenorhabditis elegans*. Both Ku70 and Ku80 possess a leucine-zipper motif, and they both have a carboxy-terminal region of ~150 amino acid residues that are important for Ku70 and Ku80 dimerization and also required for effective interactions with DNA ends. Ku70 and Ku80 cooperatively bind to DNA ends; neither subunit alone can bind to DNA effectively. Ku heterodimer also has helicase and ATPase activities, and these activities play a role in efficient DNA binding. DNA-PKcs is a member of the phosphatidylinositol-3-kinase (PI-3-K) superfamily, however, DNA-PKcs does not possess lipid kinase activity (Hartley *et al.*, 1995). The catalytic activity

of DNA-PK is triggered by association with linear DNA. After the Ku heterodimer binds to DNA ends, DNA-PKcs interacts with Ku through its carboxy-terminal quarter. Like other double stranded DNA (dsDNA) binding proteins, DNA-PKcs possesses an open channel and an enclosed cavity with three openings large enough to accommodate single stranded DNA (ssDNA) (Leuther, et al, 1999). Binding with ssDNA and dsDNA is essential for the kinase activity of DNA-PKcs.

The recruitment of DNA-PKcs after Ku binding to DNA ends can protect the ends from nucleolytic degradation; this is essential for NHEJ pathway in DNA DSBs repair. Once positioned at the DNA DSB, Ku and DNA-PKcs recruit other NHEJ factors by phosphorylation. DNA-PK can phosphorylate XRCC4 *in vitro* because XRCC4/ligase IV complex interacts with DNA-PK directly or indirectly through an unidentified intermediating kinase (Leber, et al 1998). This phosphorylation may be important for XRCC4/ligase IV activation. The MRN complex (Rad50, Mre11, and NBS1) may also activated by DNA-PK after it binds to DNA DSBs. DNA-PK may have other functions in NHEJ pathway. It may help Ku-80 to regulate a chaperone protein Hsp70 (Zhu *et al*, 1996) which can inactivate other unknown repair factors by structural modification when repair is complete though this is not firmly established. These modified repairing factors then can be removed from DNA. Also, some proteins like recombination factors which may block the repair process are also removed through the action of DNA-PK. In the NHEJ pathway, when two DNA ends are brought close

enough together, DNA-PKcs may undergo autophosphorylation and remove itself from DNA.

DNA-PK can be activated after IR or other DNA damaging agents trigger the signaling pathways that result in apoptosis or cell cycle checkpoint arrest. One substrate of DNA-PK is TP53. TP53 plays important roles in triggering apoptosis or cell cycle arrest after DNA damage. DNA-PK can phosphorylate serine 15 and serine 37 of TP53 *in vitro*, and this phosphorylation can affect the binding of TP53 to HDM2. HDM2 targets TP53 for ubiquitin-mediated proteolysis. Thus, DNA-PK phosphorylation increases the stability of TP53. DNA-PK also can directly phosphorylate HDM2, which has the effect of increasing TP53 activity since phosphorylated HDM2 cannot target TP53 for ubiquitin-mediated proteolysis (Mayo *et al.* 1997).

Ataxia-Telangiectasia

Ataxia-telangiectasia (A-T) was described as a disease by Boder and Sedgwick in 1957. A-T is typically a progressive neurodegenerative condition, inherited as an autosomal recessive disorder with a wide variety of clinical manifestations (Sedgwick and Boder, 1991). Ataxia presents when the affected child begins to walk and at about 1 year of age, the patient has postural instability of the trunk (Kuljis *et al.* 1997). When the patient gets older, the ataxia is progressive. The patient will have dystonic posturing, blinking before gaze changing and other

involuntary movement (Boder, 1985). At about 10 years of age, the patient will lose his/her mobility. Telangiectasia is another clinical manifestation, which shows later than ataxia. It is observed between 2~8 years of age. The patient will have oculocutaneous telangiectases, a butterfly pattern of telangiectases on their face, and hair-like telangiectases in the ear (Lavin and Shiloh, 1997). A-T patients suffer immunodeficiency, have increased risk of recurrent sino-pulmonary infections and a greatly increased risk of lymphoreticular malignancies. They also suffer from growth retardation, incomplete sexual maturation and endocrine abnormalities. The greatest cause of mortality in these patients is believed to be the result of atrophy of all cerebella cortical layers with extensive Purkinje and granule cells degeneration (Boder, 1985, Sediwick and Boder, 1991).

There are several fibroblast cell strains (more than 19) from genetically unrelated AT patients have been tested for their cell survival (colony-forming abilities) after exposure to X or γ -rays. All these strains showed reduced survival compared to normal controls (Cox, *et al*; 1978; Paterson *et al*; 1979). All the strains had similar increased sensitivity to irradiation, ranging from 2.7~3.4 fold above normal (Cox, *et al*; 1978). A-T strains are also hypersensitive to neutron and “far UV light-like” (300~360nm light) irradiation (Paterson *et al*; 1979, Arlett, 1977). Cells from A-T donors can be readily distinguished by distinct cytogenetic characteristics, including spontaneous and irradiation induced chromosome aberrations (German, 1972; Harnden, 1974). Various types of chromosome

aberrations (e.g. breaks, gaps, fragments, and dicentrics) are found at a greater frequency in A-T cells than in controls from normal volunteers (Harnden 1974, Oxford *et al* 1975, Taylor *et al* 1976, Cohen *et al* 1978). These spontaneous aberrations vary greatly not only among different patients (Kraemer 1977), but also within the same patient as a function of donor age (Hecht McCaw 1977) and cell type, e.g. fibroblasts versus lymphoblastoid cells (Cohen *et al* 1978). Irradiation can induce many more chromosome aberrations in A-T cells than in normal cells (Higurashi 1973). After G0/early G1 irradiation, A-T lymphocytes showed chromatid-type aberrations (gaps, breaks, and especially triradials arising from chromatid interchanges) in mitosis (Taylor *et al*, 1976). However, chromatid-type damage was seldom observed in similarly treated normal cells. A-T cells also present high frequencies of chromosome-type aberrations after G0/early G1 irradiation and chromatid-type changes after G2 irradiation (Taylor 1978).

A-T maps to chromosome 11q22-23 (Gatti, *et al.* 1988). The gene defective in A-T, *ATM*, was first cloned by Yosef Shiloh and colleagues. This gene is ~150kb in length, and it has over 66 exons (Uziel, *et al.* 1996). The protein product of this gene is ~350kDa, 3056 amino acids (Shiloh Y, 2003). More than 80% of mutations in A-T patients result in ATM protein truncations (Byrd *et al.* 1996; Gilad *et al.* 1996). ATM plays a very important role in the cellular response to DNA damage, functioning as a nuclear serine/threonine protein kinase to control cell-cycle checkpoints. The ATM response to DNA damage is very fast,

extensive and sensitive, and is mediated by phosphorylation of protein substrates or autophosphorylation. Autophosphorylation of ATM Ser-1981 is a critical step in ATM activation after DNA damage. Ser-1981 is located in the amino terminus of the FAT domain on ATM. The FAT domain has approximately 500 amino acids and it may be required for correct confirmation of the PI kinase domain (Bosotti, *et al.* 2000). To test the importance of ATM Ser-1981 phosphorylation, researchers replaced the residue with alanine (ATMS1981A), thus preventing IR-induced phosphorylation at this site. This mutant ATM protein fails to show any kinase activity in cells (Bakkenist, *et al.* 2003). *In vivo*, when ATM is not activated its kinase domain is sequestered within a domain encompassing amino acid residues 1961-2046 or forms a homodimer by binding to same region (1961-2046) on another molecule of ATM (Kitagawa, *et al.* 2005). After the Ser-1981 phosphorylation, this association is broken and the kinase domain is exposed and accessible to phosphorylate target substrates. The alanine in mutant ATM cannot be phosphorylated so the kinase domain of ATM cannot be released or activated.

ATM responds rapidly to DNA damage, and this activation of ATM is not dependent on direct binding to DNA DSBs. According to a recent model, this activation may be the result of changes in chromatin structure (Kitagawa, *et al.* 2005). After IR induction of DNA damage in cells, some aspect of the chromatin structure may change and induce an alteration in ATM conformation. This change would lead to autophosphorylation of Ser-1981 on ATM homodimers, and

the autophosphorylation would cause the dimer dissociation. After the kinase domain release, more ATM Ser-1981 would be phosphorylated in a cascade that transfers the signal of DNA damage to ATM substrates (Bakkenist, *et al.* 2003). The MRN complex (MRE11, RAD50, and NBS1) also can detect chromatin structure after IR, so this complex also directly influences the activation of ATM and its recruitment to DNA DSB. The MRN complex is also a substrate of ATM; as will be discussed below.

ATM has many substrates through which it affects cell-cycle checkpoints. It phosphorylates a serine or threonine residue only if it is followed by a glutamine (the 'SQ/TQ' motif). If there is a positively charged amino acid located next to the target serine/threonine, the phosphorylation will be diminished. If the amino acid next to target serine/threonine is hydrophobic or negatively charged, phosphorylation will be enhanced (Kim, *et al.* 1999). TP53 is a transcription factor that plays a major role in cell cycle arrest. ATM activates TP53 by phosphorylating it at Ser-15, thus increasing its stability and abundance. TP53 upregulates transcription of p21, an inhibitor of cyclin E and CDK2. The cyclin E and CDK2 complex is essential for cell cycle progression from G1 to S phase (Giaccia, *et al.* 1998). DNA damage caused cell cycle arrest at the G1 checkpoint because of increased cellular levels of TP53, which is also mediated through ATM phosphorylation. The reason is, ATM can phosphorylate HDM2 at Ser-395 which decreases its ability to bind to TP53. HDM2 controls cellular levels of TP53 through degradation; it binds to TP53 and targets it for ubiquitin-mediated

proteolysis (Haupt, *et al.* 1997; Kubbutat, *et al.* 1997). So, after phosphorylation, HDM2 cannot target TP53 for ubiquitin-mediated proteolysis, (Mayo *et al.* 1997), thus TP53 level increases.

In patients with ataxia-telangiectasia, poor induction of TP53 after IR has been observed. Ser-20 on TP53 also can be phosphorylated after radiation-induced DNA damage, and this phosphorylation is indirectly controlled by ATM. *In vitro*, CHK2 can phosphorylate TP53 on Ser-20 (Hirao, *et al.* 2000; Chehab, *et al.* 2000; Shieh, *et al.* 2000), and CHK2 is a substrate of activated ATM (Matsuoka, *et al.* 1998; Zhou, *et al.* 2000).

ATM can also control the S-phase checkpoint by phosphorylating the MRN complex. Researchers found that ATM can phosphorylate NBS1 on Ser-343 *in vivo*, and MRE 11 also contains an ATM target site (Lim, *et al.* 2000; Gatei, *et al.* 2000; Zhao, *et al.* 2000; Wu, *et al.* 2000; Kim, *et al.* 1999). These phosphorylations may be required for the IR induced S-phase checkpoint. BRCA1 is also an important substrate of ATM. *In vivo*, BRCA1 can bind to RAD51 to form a complex which is essential for homologous recombination. Cells lacking BRCA1 will be hypersensitive to IR and defective in homologous recombination. ATM can phosphorylate CtIP (CtBP-interacting protein) which can bind to BRCA1 and inhibit its function. This phosphorylation of CtIP will release and activate the BRCA1.

In the mouse, an *ATM* homolog, *Atm* has been identified and mapped 30 cM from the top of mouse chromosome 9. Mouse *Atm* shares 84% amino acid identity and

91% similarity with ATM in human. *Atm* knockout mice have been created by several groups and model some aspects of human A-T. *Atm* deficient mice suffer growth retardation, even though their growth rate is almost normal they are 10~25% smaller and lighter than wild type mice of the same sex (Barlow, *et al.* 1996; Xu, *et al.* 1996; Elson, *et al.* 1996). *Atm*^{-/-} embryo fibroblasts grow slowly in tissue culture and reach a senescence-like growth arrest after only a few passages (Barlow, *et al.* 1996; Xu, *et al.* 1996). *Atm* deficient mice are infertile, because their sex gonads are extremely small and show a complete absence of mature gametes (Barlow, *et al.* 1996; Xu, *et al.* 1996). This infertile problem may be caused by a meiotic arrest at the zygotene-pachytene stage of prophase I (Xu, *et al.* 1996; Barlow, *et al.* 1997). *Atm* deficient mice also suffer immunologic abnormalities and cancer predisposition. *Atm*^{-/-} mice have normal lymphoid organ structure, however, these organs are smaller than those of normal mice, and the number of thymocytes is reduced (Barlow, *et al.* 1996; Xu, *et al.* 1996). Researchers believe that the defective V(D)J recombination process in *Atm*^{-/-} mice is responsible for its abnormal maturation of lymphocytes (Xu, *et al.* 1996). A lot of *Atm*^{-/-} mice develop malignant thymic lymphomas by the age of four months to ten months ((Barlow, *et al.* 1996; Xu, *et al.* 1996; Jacks, *et al.* 1994). Hypersensitivity to radiation is observed in *Atm*^{-/-} mice, and this may be resulted from radiation toxicity to the gastrointestinal tract (Barlow, *et al.* 1996). *Atm*^{-/-} mice are impaired in several motor function tests, such as the rota-rod and open field tests (Barlow, *et al.* 1996). And these mice also have much shorter stride

lengths than wild type mice (Barlow, *et al.* 1996). All of these suggest neurological deficiencies in *Atm*^{-/-} mice, however, no histological abnormalities were observed in the brains of *Atm*^{-/-} mice (Barlow, *et al.* 1996; Xu, *et al.* 1996). This is the biggest problem of the *Atm* knockout mouse as a model for human ataxia-telangiectasia patients.

Assays of cellular radiosensitivity

Clonogenic Survival

Cell survival curves describe the relationship between the radiation dose and the proportion of cells that survive. For cells cultured *in vitro*, survival is defined by reproductive integrity. Reproductively dead cells may persist in culture as intact cells able to make proteins or DNA, and they may be able to go through one or two mitoses; however, these cells have lost the capacity to generate enough to give rise to a colony.

A traditional *in vitro* clonogenic survival assay uses adherent cells from an actively growing stock culture. At near confluence, the cells are blocked in the G0/G1 phase of the cell cycle by culture in isoleucine free medium for 48 hours. The cells are then irradiated. After detachment with trypsin, these cells are counted (with an electronic particle counter or hemocytometer); then a defined number of cells are plated into new dishes. After incubation (about 1~4 weeks), each single cell will divide several times and form a colony which is visible to the naked eye. All the cells making up each colony are the

progeny of a single ancestor. Control groups (cells not exposed to irradiation) are used to calculate plating efficiency. For irradiated groups, they will be exposed to irradiation, and then cells in these groups may perform differently. Some of the irradiated cells may never enter mitosis; they may even undergo apoptosis. Some cells may complete one or two divisions and form a tiny colony; they are considered reproductively dead. Some cells may grow into large colonies which differ little from unirradiated controls indicating cell survival. Surviving colonies are counted and the surviving fraction is calculated from the colony count and plating efficiency. The process is repeated for a range of doses and cell survival curves are generated from surviving fractions data at different doses of irradiation (Hall, E; et al, Radiobiology for the radiologist, sixth edition, 2006).

Surviving Fraction at 2 Gy (SF2)

Radiotherapy is a major modality of cancer treatment. Radiotherapy damages normal tissues in the irradiated field. Individual patients have different sensitivities to radiation-induced normal tissue injury. Presently, complication risks for an individual irradiated patient can be predicted only by the complication rates seen in similar populations. The standard dose for a population may be too low for some patients whose tumors are very resistant. Nevertheless, the same dose may present an unacceptable risk of complication for patients whose normal tissues are very sensitive (Peters, L et

al; 2001). Predicting normal tissue and tumor radiosensitivity for individual patients is an important area of research because it would allow radiotherapy treatment planning to be individualized, increasing cure rates while decreasing complication rates.

One assay that has been investigated for its use in predicting normal tissue response is the SF2 (surviving fraction after 2 Gy) assay (Ismail, S and Brock, WA; 2004). The assay is essentially a truncated clonogenic survival curve using patient fibroblasts that is limited to the 2 Gy dose. A 2Gy exposure was chosen because curative radiotherapy is typically delivered using a daily fraction size of 1.8~2.0Gy. A major drawback that limits the clinical application of this assay is that it takes too long to run. It may take weeks to grow fibroblasts from punch biopsies and then determine their SF2. Generally, treatment cannot be delayed for this length of time (Story, MD and Brock, WA; 2004).

Low dose rate survival

Using low dose rate exposures rather than acute exposures (for example, 3mGy/hr in place of 60Gy/hr) may have some advantages in assessing radiosensitivity in cell survival assays, (NCRP 1980; Amdur and Bedford 1994; Vilenchik et al, 2000). When dose-rate is lowered, the density of particle hits to the cell nucleus per unit time decreases, and the amount of DNA damage present at a given time is lower. A cell in which several DNA

DSB occur concurrently is more likely to sustain chromosomal aberrations than one in which there is only one DSB. By delivering dose over an extended time period repair of a given DSB may be repaired before another is generated thus diminishing opportunities for interchromosomal exchanges (Sax, 1940; Catcheside, et al., 1946).

γ -H2AX

In eukaryotes, DNA is highly condensed to form chromosome, and nucleosome is the fundamental subunit of the chromosome. Within each nucleosome, 146 bp of DNA are wrapped 1.7 times around a central protein core. This central protein core is composed by eight histone molecules (an octamer) include two H2A/H2B dimers and a (H3/H4)₂ tetramer (Luger K, 2003). Each histone in this octamer contains a globular domain which is important for histone-histone and histone-DNA contact. They also have a tail motif in both the COOH- and NH₂-terminals. H2AX is one of the H2A subfamily, and it has a different primary structure and/or amino acid sequence (Lewis, et al. 2003). The H2AX gene has been localized by fluorescence in situ hybridization to chromosome 11q23.2-q23.3, away from the known clusters of human histone genes on chromosomes 1, 6, and 12 (Ivanova, *et al.* 1994). In normal human fibroblast, H2AX composes about 10% of the H2A histone. This level can vary from 2~25% depending of the cell line or different tissues. For human fibroblast, a cell contains about 6×10^6 molecules of H2AX (Rogakou, *et al.* 1998). In cells, H2AX

can distribute to the whole genome and it contains a longer COOH- terminal region than other H2A species. γ -H2AX is the phosphorylated form of H2AX, and the phosphorylated site, Ser-139, is very important for its function. This induction may be mediated by ATM and DNA-PK (Stiff, *et al.* 2004). For ATM phosphorylation process, NBS1 C- terminal is required to interact with ATM, and then H2AX can be phosphorylated by ATM in nucleus. When ATM and/or NBS1 C -terminal region is absent, DNA-PK can phosphorylate H2AX without ATM and/or NBS1 (Stiff, *et al.* 2004). H2AX also can be phosphorylated at Ser-1, acetylated on Lys-5 and ubiquitinated on Lys-119 (Wu R.S., *et al.* 1986).

We believe DNA DSBs can induce γ -H2AX. γ -H2AX can be detected in three minutes after IR, and it can reach the highest level in 10~30 minutes after irradiation (Rogakou, *et al.* 1998). After IR, H2AX in a large region can be phosphorylated, this may contain two megabases of chromatin or thousands of nucleosomes (Rogakou, *et al.* 1998). By using anti- γ -H2AX antibody, researchers found that H2AX can be massively phosphorylated very close to DSBs and these γ -H2AX can form nuclear foci (Oliver, *et al.* 1997). There is a 1:1 relationship between γ -H2AX foci and the number of DSB (Weber, *et al.* 1993), also because γ -H2AX can be induced very fast after IR, γ -H2AX recognizing antibodies can be a very acute way to quantify the presence of DNA DSBs.

There are several evidences showed that γ -H2AX is required for accumulation of DNA damage repair factors, like 53BP1, NBS1, BRCA1 and MDC1 (Paull, *et al.*

2000; Stewart, *et al.* 2003; Celeste, *et al.* 2002; Bassing, *et al.* 2002). γ -H2AX also can directly interact with 53BP1, NBS1 and MDC1 (Stewart, *et al.* 2003; Ward, *et al.* 2003; Kobayashi, *et al.* 2002; Xu, *et al.* 2003). For NHEJ and/or HR pathways in mammal cells, H2AX phosphorylation is not essential, but it can modulate both pathways (Reina-San-Martin, *et al.* 2003; Peterson, *et al.* 2001). By increasing the concentration of repair factors at DSBs, γ -H2AX may help to assemble functional repair complex at DNA damage. H2AX defection may affect G2/M phase cell cycle checkpoint response. Without γ -H2AX, 53BP1 may not accumulate at DSBs efficiently, and this will cause the failure of G2/M phase cell cycle checkpoint response (Fernandez-Capetillo, *et al.* 2002; DiTullio Jr, *et al.* 2002; Wang, *et al.* 2002).

H2AX deficient can cause growth defect, and this is already been proved by H2AX^{-/-} mice. These mice are smaller in size than the normal ones and their embryonic fibroblasts also exhibit impaired growth (Celeste, *et al.* 2002). This retardation can be found after 3~4 passages in tissue culture (Celeste, *et al.* 2002). γ -H2AX plays a physiological role in sex chromosomes. In H2AX-deficient spermatocytes, X- and Y- chromosomes cannot condense to form a sex-body, so that they cannot initiate meiotic sex chromosome inactivation (Fernandez-Capetillo, *et al.* 2003). Then, this function lost can cause severe defects in the pairing of X-Y chromosomes.

The result about loss of H2AX is always genomic instability, and this always can cause cancer development. However, there is no apparently increase in tumor

development in H2AX^{-/-} mice (Celeste, *et al.* 2003; Bassing, *et al.* 2003). Another DNA damage sensor, TP53, may explain this conflict. TP53 protein can arrest cell division or trigger apoptosis when genomic instability happened, even without γ -H2AX. However, if TP53 is deficient and H2AX level is lower than wild type level (H2AX^{+/-} TP53^{-/-} mice), cell cannot maintain genomic stability. Under this situation, the insufficient of γ -H2AX (even it exist in cells) will case reduced growth rate and radiation sensitivity (Celeste, *et al.* 2003; Bassing, *et al.* 2003). So, we can say that H2AX functions as a dosage-dependent tumor suppressor. Except DNA DSBs, γ -H2AX also accumulate at sites of V(D)J recombination in developing thymocytes (Xu, *et al.* 2003).

H2AX phosphorylation (γ -H2AX foci) can be used as a biodosimeter for DNA damage in cells exposed to irradiation. Un-repaired DNA DSBs can be detected as distinct γ -H2AX foci in eukaryotic cells (Rothkamm et al, 2003; Rogakou, et al, 1999). Typically γ -H2AX foci are quantified by immunofluorescence using antibodies directed against γ -H2AX. The kinetics of γ -H2AX appearance and persistence after irradiation are related to radiosensitivity. For example, the assay can be used to distinguish *Atm*^{+/-} from *Atm*^{+/+} cells after low dose-rate irradiation (Kato and Bedford, 2006). This study showed that DNA repair deficient mutants show higher residual levels of γ -H2AX foci after irradiation exposure.

G2 Chromosomal Radiosensitivity

Chromosomal aberration analysis is one of the most reliable and sensitive methods of measuring radiation-induced damage. There are two kinds of chromosomal aberrations: chromosome aberrations and chromatid aberrations. If a cell is irradiated before its chromosome material has been duplicated, chromosome aberrations are always happened. If a cell is irradiated at later interphase (G2), after DNA materials doubled and the chromosomes consist of two strands of chromatin, and then the aberrations are called chromatid aberrations. We use G2 chromosomal aberration analysis in our experiment, and most damages are chromatid aberrations. Analysis chromosomal damage in G2 phase may reduce some of these problems and make a more accurate determination of cytogenetic effects following irradiation (Kawata, T; et al, 2004). Now, Chromosomal aberration assays in human peripheral blood lymphocytes have been used and they may provide a valid method for the detection of radiation exposure (Vral, A; et al 2004). Some individuals in the normal population may have increased risks for the development of cancer, and to identify these individuals may be very difficult. The potential of chromosomal aberration assays may solve this problem because researchers have detected chromatid breaks in G2 cells in a significant proportion of cancer patients (Baeyens et al., 2002; Baria et al., 2001; Baria et al., 2002; Parshad et al., 1996; Riches et al., 2001; Roberts et al., 1999; Rothfuß et al., 2000; Scott et al., 1998; Scott et al., 1999 and Terzoudi et al., 2000).

An initial study found that peripheral blood lymphocytes from breast cancer patients irradiated in G2 phase of the cell cycle had higher levels of chromosomal aberrations than lymphocytes of healthy controls (Scott et al, 1994). Separate studies on an additional 50 patients using the G2 assay showed that 30%-40% had an elevated sensitivity compared to controls (Scott et al, 1998).

Recombinant Inbred Mice

Recombinant inbred (RI) strains contain unique, approximately equal proportions of genetic contributions from two progenitor inbred strains. RI strains are constructed by crossing two inbred strains to produce an F1 generation, followed by 20 or more consecutive generations of brother x sister mating (Bailey 1971; Taylor 1978). Multiple RI strains comprise RI strain panels. In each RI strain, about 50% of the genome is derived from each parental strain. Also, the RI strains should be homozygous at every locus though in reality small regions of heterozygosity persist in some strains.

RI strains have a number of advantages over F2 and backcross populations for some applications, especially for mapping genes, because inbreeding beyond the F2 generation fosters additional opportunities for recombination between linked genes, a given number of RI strains can provide higher mapping resolution than can the same number of F2 mice. RI strains are renewable because they are inbred. After a mouse been sacrificed in an *in vivo* experiment, it can easily be replaced. Researchers can compare their results with information published on

the same set of RI strains and the data for the strains is cumulative allowing for correlation of traits measures in different laboratories at different times. Data obtained from several RI strain sets may be compared or combined, particularly if the sets have a progenitor strain in common or are assorting for alleles of common origin in the genomic region(s) of interest.

For radiation carcinogenesis research two RI panels are of particular interest: the CXB strain set and the BXH strain set. In each of these strain sets the progenitor strains have been well characterized for radiogenic cancers. In our research, we are using CXB RI strains. The CXB RI strain set consists of 13 RI strains derived from matings of BALB/cBy (C) and C57BL/6By (B) mice. The CXB progenitor strains differ in their susceptibility to radiation-induced mammary tumors with BALB/c being susceptible and C57BL/6 being resistant (Storer, Mitchell and Fry). In part, the susceptibility difference can be explained by polymorphisms in the *Prkdc* gene which encodes the catalytic subunit of DNA-dependent protein kinase (Ullrich, Yu etc). The BALB/c allele of the *Prkdc* gene encodes a hypomorphic variant of DNA-PKcs responsible for defective DNA DSB rejoining in that strain.

The first set of CXB RI strains were developed by Dr. Donald Bailey and moved to the Jackson Laboratory (JAX) in 1967. So, these first set of CXB RI strains are designated as CXB-strain number/ByJ where “By” is Bailey’s lab code and “J” is the JAX lab code. Later, Dr. J. Hilgers at the Netherlands Cancer Institute in Amsterdam and Dr. L. Mobraaten at JAX lab developed additional CXB strains,

and these strains are named as CXB-strain number/HiAJ. These combined sets of CXB RI strains contain 13 different strains in total. All these CXB RI strains are highly inbred; all of them have been inbred over 70 generations (some of them over 130 generations).

Correlating Traits in Genetically Randomized Populations

RI strains have unique patterns of genetic randomization, so then can be used to measure tendencies of genetic characters to cosegregate. Also, RI strains have systematical characters because they are inbred and genetically defined populations, so they can be used on repeated assays (Bailey 1981).

In our experiment, we use CXB RI strains mouse cells reaction under different irradiation dosage as a model of network analysis. The relationships between cell survival rate under irradiation and γ -H2AX foci numbers under irradiation will be tested in our experiment.

Materials and Methods

1. Cell culture

Mouse fibroblast cultures (generously provided by Dr. H. Nagasawa) were initiated from liquid nitrogen stocks frozen in 10% DMSO/90% cell culture medium at the lowest passage number available (all <3). The cells were cultured in minimum essential medium (MEM, HyClone, HyQ, #SH30008-03) supplemented with 15% Fetal Bovine Serum (JRH biosciences, #12303-500M), 100U/ml penicillin G (Sigma), 100ug/ml streptomycin sulfate (Sigma) and 0.5ug/ml Fungizone (Amphotericin B, GIBCO, #15290-018). The frozen stocks were thawed in a 37 °C water bath and one to two ml of the thawed fibroblast suspensions were diluted with 5ml of fresh cell culture medium. The cell suspension was then centrifuged at 1000rpm for 5 minutes at room temperature. After centrifugation, the supernatants were discarded and the cell pellets resuspended in one ml of fresh cell culture medium. These suspensions were then aliquoted into P-25 tissue culture dishes (Fisher Science) containing 5ml fresh cell culture medium (medium filled P-25 dishes are placed in a 37 °C incubator supplied with 95% air/5%CO₂ mixture for at least one hour to equilibrate before plating the cells). Culture medium was changed the next day. The cells were passaged until they recovered from cryopreservation (fewer than 6 passages) before they were used for the experiments.

2. Acute dose irradiation

Fibroblasts were subcultured into P-100 cell culture dishes (Fisher Sciences) filled with 10 ml fresh, pre-equilibrated cell culture medium and grown in a 37°C incubator supplied with 95% air/5%CO₂ mixture. After the cells reached 75% confluence, usually within 4~5 days following subculture, the cell culture medium was replaced with 10 ml of isoleucine free cell culture medium supplemented with 10% Fetal Bovine Serum (JRH biosciences, #12303-500M), 100U/ml penicillin G (Sigma), 100ug/ml streptomycin sulfate (Sigma) and 0.5ug/ml Fungizone (Amphotericin B, GIBCO, #15290-018). The cells were incubated for 24 hours and then the media was replaced with fresh isoleucine free medium. Twenty-four hours after the final media change, the P-100 dishes were transported to the MRB470 irradiation facility. Cells were irradiated at room temperature with graded doses of 0 (control) to 600cGy of ¹³⁷Cs 662 keV gamma-rays at a dose rate of 250 cGy/min, in a J. L. Shepard and Associate Mark I-68A beam irradiator with an approximate activity of 3170 Ci (as of September 2004). After irradiation, the medium was aspirated immediately and the cells were detached with 0.25% trypsin/EDTA (GIBCO) in Ca²⁺/Mg²⁺-free PBS for three minutes at 37 °C. One ml of the single cell suspension was diluted into 9 ml of PBS and counted with a Coulter Z-1 cell counter (Beckman-Coulter, Inc.). Cells were then plated at low density in P-100 dishes containing pre-equilibrated medium to achieve approximately 50~100 viable colonies for each dose point. After plating, the dishes were returned to the incubator and the medium was fully

replaced after ten days of growth. Three weeks post-irradiation, the colonies were aspirated, rinsed with 0.9% sodium chloride and fixed with 100% ethanol. The dishes were then stained with a 0.1% crystal violet/methanol solution and colonies with >50 viable cells were counted.

3. Low Dose Rate Irradiation

Fibroblasts were subcultured in P-25 cell culture dishes filled with 5 ml fresh cell culture medium (pre-equilibrated in 37° C incubator supplied with 95% air/5%CO₂ mixture for at least one hour). After the cells reached 75% confluence, usually within 2 to 3 days following subculture, the medium was aspirated and the cells were detached with 0.25% trypsin/EDTA (GIBCO) in Ca²⁺/Mg²⁺-free PBS for three minutes at 37° C. One ml of the single cell suspension was diluted into 9 ml of PBS and counted with a Coulter Z-1 cell counter (Beckman-Coulter, Inc.). Cells were then plated at different numbers (200 to 2x10⁴) in P-100 dishes containing pre-equilibrated medium to achieve approximately 50 to 100 viable colonies for each dose point following three weeks of growth. After plating, the dishes were transferred to a 37 °C incubator supplied with 95% air/5%CO₂ mixture in MRB008 and incubated for 4 hours to allow for cell attachment prior to initiating irradiation. The cells were continuously irradiated for 7 days (168 hours) at the dose rates indicated in Figure 2-1. After 7 days, the dishes were removed from irradiation facility and transferred to 37 °C incubator supplied with 95% air/5%CO₂ mixture for another 3 days (72 hours), the medium was

then exchanged with fresh cell culture medium. After another 10 days of growth, the culture media was aspirated. Dishes were rinsed with 0.9% w/v sodium chloride, fixed with 100% ethanol and stained with 0.1% w/v crystal violet/methanol solution. Colonies with >50 viable cells were counted.

The MRB008 facility is equipped with a J. L. Sheperd and Associates Model 81-14 beam irradiator containing a single ~21 Ci ¹³⁷Cs source placed approximately 100 cm above a 37 °C incubator. The incubator is set on a hydraulic lift so it can be raised or lowered to vary the dose rate. Four shelves are available in the MRB008 incubator with sufficient space to hold up to 72 P-100 dishes per shelf.

4. γ -H2AX Analysis Following Acute Exposure

The fibroblasts were subcultured into 2 well Lab-Tek II chamber slides (Nalge Nunc International) filled with 2ml fresh pre-equilibrated cell culture medium. After the cells reached 50% confluence, usually within 1 to 2 days following subculture, the media was replaced with 2 ml isoleucine free cell culture medium. The cells were incubated in a 37 °C incubator supplied with 95% air/5%CO₂ mixture for 24 hours, then the media was replaced with 2 ml of fresh isoleucine free cell culture medium. Twenty-four hours after the final medium change, the cell culture chamber slides were transported to the MRB470 irradiation facility. Cells were irradiated at room temperature with dose of 100cGy of ¹³⁷Cs 662 keV gamma-rays at a dose rate of 250 cGy/min, in a J. L. Shepard and Associate

Mark I-68A beam irradiator with an approximate activity of 3170 Ci (as of September 2004). After irradiation, cells were transferred back to a 37 °C incubator supplied with 95% air/5%CO₂ mixture. After one hour of incubation, the cells were washed with ice cold Ca²⁺/Mg²⁺-free PBS twice and fixed in 4% paraformaldehyde (J. T. Baker) in PBS at 4 °C. The cells were rinsed with PBS twice, then treated with 0.2% Triton X-100 (Sigma) in PBS for 5 min at room temperature. Before immunocytochemical detection of γ -H2AX, cells were blocked with 10% goat serum (Abcam) in PBS overnight at 4 °C to reduce non-specific antibody binding.

The primary antibody (anti- γ -H2AX, Trevigen, 4411-PC-100) was diluted 1:500 in PBS with 10% goat serum. Five hundred μ l of the primary antibody solution was placed in each chamber and the chamber slides were then incubated at 37 °C for 1 hour. The cells were then rinsed twice with PBS and then given three 15 minute PBS washes. The secondary antibody (Invitrogen, A11008, goat anti-rabbit conjugated to 488 Alexa Fluor) was diluted 1:1000 in PBS with 10% goat serum. One ml of the secondary antibody solution was added to each chamber, then the chamber slides were incubated at 37 °C for 1 hour. Cells were then rinsed with PBS two times, and washed with PBS three times, 15 minutes each. The slides were mounted in a solution of 1.5 μ g/ml DAPI containing slow-fade (Invitrogen, P36931).

Images of cells were obtained using an Olympus AX-70 fluorescence microscope equipped with a PSI image analysis system utilizing the MAC-Probe package.

There was often some non-specific background signal over and between cells that was smaller and less intensely fluorescent than the γ -H2AX foci. Cell images were stored and foci numbers were scored later. Only the smaller cell nuclei were scored and the occasional larger nuclei were ignored. Samples were coded so the scorer did not know their origin.

5. γ -H2AX formation under low dose-rate

Fibroblasts were subcultured into 2 well Lab-Tek II chamber slides (Nalge Nunc International) filled with 2ml fresh, pre-equilibrated cell culture medium/chamber. After the cells reached 90% confluence, usually within 1~2 days following subculture, the chamber slides were transferred to a sealed box which filled with a 95% air/5%CO₂ mixture. The box containing the chamber slides was placed in the low dose rate irradiation facility in MRB012. After 24 hours exposure at a dose rate of 10.2cGy/hour, the cells were quickly (within 5 minutes) washed twice with ice cold Ca²⁺/Mg²⁺-free PBS and fixed with 4% paraformaldehyde (J. T. Baker) in PBS at 4 °C, for 10 minutes. The cells were rinsed with PBS twice and then treated with 0.2% Triton X-100 (Sigma) in PBS for 5 min at room temperature. Before immunocytochemical detection of γ -H2AX, cells were blocked with 10% goat serum (Abcam) in PBS overnight at 4 °C to reduce subsequent non-specific antibody binding.

The primary antibody (anti- γ -H2AX, Trevigen, 4411-PC-100) was diluted 1:500 in PBS with 10% goat serum. Five hundred ul of the primary antibody solution

was placed in each chamber and the chamber slides were then incubated at 37 °C for 1 hour. The cells were then rinsed twice with PBS and then given three 15 minute PBS washes. The secondary antibody (Invitrogen, A11008, goat anti-rabbit conjugated to 488 Alexa Fluor) was diluted 1:1000 in PBS with 10% goat serum. One ml of the secondary antibody solution was added to each chamber, then the chamber slides were incubated at 37 °C for 1 hour. Cells were then rinsed with PBS two times, and washed with PBS three times, 15 minutes each. The slides were mounted in a solution of 1.5ug/ml DAPI containing slow-fade (Invitrogen, P36931).

Images of cells were obtained using an Olympus AX-70 fluorescence microscope equipped with a PSI image analysis system utilizing the MAC-Probe package. There was often some non-specific background signal over and between cells that was smaller and less intensely fluorescent than the γ -H2AX foci. Cell images were stored and foci numbers were scored later. Only the smaller cell nuclei were scored and the occasional larger nuclei were ignored. Samples were coded so the scorer did not know their origin.

The MRB012 facility consists of a custom-built 79cm-diameter array of twelve ^{137}Cs sources housed in a 37 °C warm room without a CO₂ supply. The activity of each ^{137}Cs source is approximately 2.2 mCi. The sources are attached to the ends of steel cables that are routed through a series of copper tubes into the MRB012 warm room. This system allows the sources to be retracted into shielding or extended under a 107.5 x 96.6 cm shelf in the warm room by pushing or pulling

the steel cables. A locked cabinet with the cable controls is located in the MRB010. The total available shelf surface for cells is approximately 4.6 m².

6. G2 Chromosome Analysis

The G2 assay data were collected by Dr. H. Nagasawa and Mr. A. Roby. Fibroblasts were cultured into P-100 cell culture dishes (Fisher Sciences) filled with 10 ml of fresh cell culture medium supplemented with 1X GlutaMAX™-I (L-alanyl-L-glutamine, GIBCO/Invitrogen) and incubated at 37 °C in a 95% air/5%CO₂ mixture. The cell culture medium was replaced one day prior to irradiation. On the day of irradiation, the P-100 dishes were transported to the MRB470 irradiation facility. The cells were irradiated at room temperature with dose of 0.5Gy of ¹³⁷Cs gamma-rays at a dose rate of 250 cGy/min in a self-shielded J. L. Shepard and Associate Mark I-68A beam irradiator. After irradiation, dishes were transferred back to a 37 °C incubator supplied with 95% air/5%CO₂ mixture. Thirty minutes later, 0.1 ug/ml colcemid (GIBCO/Invitrogen) was added to the cultures and the dishes were incubated for another 60 minutes. Ninety minutes after irradiation, the media was aspirated and the cells were detached with 0.25% trypsin/EDTA (GIBCO) in Ca²⁺/Mg²⁺-free PBS for three minutes at 37 °C. The single cell suspension was transferred into a 15ml conical tube and centrifuged for 5 minutes at 1000 rpm at room temperature. After centrifugation, the supernatant was decanted and the cell pellet was gently broken up. The broken cell pellet was resuspended in 10 ml of 37 °C, 75mM KCl

hypotonic buffer, and the tube was incubated in a 37 °C water bath for 7.5 minutes. Two ml of freshly prepared fixative (3:1 methanol:acetic acid) was added into cell suspension, and the tube was gently inverted to mix the solutions. After incubation at room temperature for 2.5 minutes, the cell suspension was centrifuged for 4 minutes at 1000 rpm at room temperature. The supernatant was poured into a hazardous waste container and the cell pellet was gently disaggregated. Three to four ml of fresh fixative was added to the cell suspension and mixed by repeated passage through a pipette. The cell suspension was placed into a cold room (4 °C) for 7 days. It was then returned to room temperature and centrifuged at 1000 rpm for 5 minutes. The supernatant was poured into a hazardous waste container and the cell pellet was gently broken up. Three to four ml fresh fixative was dropped into cell suspension and the cells were further resuspended by pipetting. After five minutes, this centrifuge and fixation process was repeated once more. The cell suspension was resuspended in 0.5 to 1.5 ml of fresh fixative (depending on the volume of the cell pellet) after centrifugation. Sixty µl of the cell suspension was dropped onto a clean, cold and wet microscope slide. The slide was air dried and placed in 37 °C warm room overnight. After this, the slide was stained in a 10% Giemsa solution for 15 minutes at room temperature. Then, the slide was washed in McIlvaine's rinsing buffer (0.1 M citric acid and 0.2 M disodium phosphate at pH 7.0) and distilled water, and air dried. The slide was stored at 37 °C overnight, and then was sealed at room temperature with Cytoseal 60 mounting medium and a 24mm x 55mm

glass coverslip.

7. Genotyping

Cells were detached with 0.25% trypsin/EDTA (GIBCO) in Ca²⁺/Mg²⁺-free PBS for three minutes in 37 °C, and centrifuged at 1000rpm for 5 minutes, room temperature. The supernatant was discarded and the cell pellet was resuspended in 200ul PBS. DNA was extracted from cells using the DNeasy tissue kit (Qiagen, #69506), according to the manufacturer's instructions. PCR amplifications were carried out using Qiagen Taq mix PCR kit (Qiagen, 201443) in a Perkin-Elmer 9600 thermal cycler (Norwalk, CT). The primer sequences used to amplify the R2140C region were: (Forward) GCCATGATCCTTAGCAAGTG and (Reverse) GCCTAAGGTAAGGTGCTGTA. PCR cycling conditions were 94°C for 30 s, 49°C for 30 s, and 72°C for 30 s for 40 cycles, followed by a final extension at 70°C for 10 min. The PCR product was digested with BsmBI (New England) at 55°C for 3 h according to the manufacturer's instructions. The restriction enzyme digestion products were separated by gel electrophoresis. In this step, 2% agarose in TAE buffer was used and the gel was run in TAE buffer at 70 volts for 40 to 50 minutes. Syber gold was used to stain the digestion products, and the gel was imaged in Kodak EDAS 290 UV camera system in Dr. Robert Ullrich's laboratory.

Results

Prkdc Genotyping

We set out to characterize several radiobiological endpoints in fibroblasts derived from the CXB recombinant inbred strain panel. The CXB progenitor strains, BALB/c and C57BL/6, differ in their susceptibility to radiation-induced mammary tumors and this difference is thought to be due, in part, to a hypomorphic allele of *Prkdc* found in BALB/c. Since *Prkdc* encodes DNA-PKcs, a component of the NHEJ DSB repair pathway, cells with the hypomorphic allele are likely to be radiosensitive in some assays. Therefore, we began by genotyping the CXB RI strain panel for the R2140C *Prkdc* polymorphism using PCR-RFLP assays (Figure 1). We found that CXB1, 3, 5, and 10 have the common (C57BL/6-like) allele and all the remaining strains have the BALB/c variant of *Prkdc*.

Clonogenic Survival

Figure 2 graphs the surviving fraction of the various fibroblast strains following acute exposure to ^{137}Cs γ -rays (2.5Gy/min). The D0 values are presented in Table 1. Because some of the survival curves of the individual strains cross one another it is difficult to precisely group the strains in this assay. However, by visual inspection of Figure 2 it appears that the most radioresistant strains are C57BL/6 and CXB1, 3 5 and 9. The large shoulder in their survival curves is traditionally

considered a marker of effective repair processes.

Conversely, the BALB/c fibroblasts are the among the most sensitive of all the strains we assayed for clonogenic survival following acute dose irradiation along with fibroblasts from CXB7, 8 and 12. All have similar D0 values and their survival curves have almost no shoulder, suggestive of ineffective repair.

Fibroblasts from the remaining CXB strains have survival curves indicating radiosensitivity intermediate between BALB/c and C57BL/6, though CXB2 and 10 are C57BL/6-like at the highest dose assayed. Most of these intermediate curves do not appear to have shoulders; however, additional data at lower doses would be needed to better define this region of the dose-response curve.

SF2

The surviving fraction at 2 Gy taken from the clonogenic survival data above is presented in Table 3.

Survival at Low Dose Rate

Cellular responses to radiation often depend on the rate at which the radiation dose is delivered. Figure 3 presents data on the surviving fraction of the different CXB fibroblast strains under low dose irradiation (1.22 to 2.66cGy/hour) and Table 2 lists the doses at which 50% survival occurred. The C57BL/6 fibroblasts were among the most radioresistant in this assay along with fibroblasts from CXB1, 3, 5 and 10.

Fibroblasts derived from BALB/c mice are nearly the most sensitive to the low dose rate irradiation. Four other fibroblast strains have a radiosensitivity similar to that of BALB/c fibroblasts; these are derived from CXB7, 8, 9 and 12.

There are other five fibroblast strains, those from CXB2, 4, 6, 11 and 13, are intermediate in sensitive to low dose rate irradiation falling between BALB/c and C57BL/6.

Acute dose γ -H2AX Focus formation

After varying doses (0 to 6 Gy) at an acute dose-rate of 2.5Gy/minute, γ -H2AX foci were scored in fibroblasts from the CXB strains (Figure 4). The results are summarized graphically in Figure 5 and the mean values are summarized in Table 1. Visual inspections of histograms of foci per cell reveal that the distributions are not Poisson. In Figure 6, the mean number of γ -H2AX foci per cell are displayed as box plots and the plots are arranged in order of increasing numbers of foci/cell. The *Prkdc* genotype of each fibroblast strain is included in this figure. It is obvious that the *Prkdc* genotypes have no relationships with γ -H2AX foci/cell. There are no clearly separated groups in this Figure. A one-way analysis of variance of the 15 strains confirmed that not all the means are equal when alpha is set at 0.05. Further comparisons with Tukey's test do not yield distinct non-overlapping groups.

Based on the observations of others, we suspect that the kinetics of appearance and disappearance of the γ -H2AX foci may differ between the fibroblast strains.

Consequently, by selecting one time point (1 hour after irradiation) we may have missed differences between the CXB strains for this endpoint following acute dose irradiation.

Low dose rate γ -H2AX Foci

After a continuous exposure of the CXB fibroblasts for 24 hours at a low dose-rate of 10cGy/hour, γ -H2AX were scored (Figure 7). The distributions of the foci in each of the strains are summarized graphically in Figure 8 and the mean values are summarized in Table 2.

The mean values for CXB 1, 3, 5, 10 and C57BL/6 fibroblasts are similar at around 4 γ -H2AX foci per cell. CXB 7, 8, 9, 12, 13 and BALB/c fibroblasts had mean values of γ -H2AX foci of around 13 per cell. CXB 2, 4, 6 and 11 had 8 γ -H2AX foci per cell, between the C57BL/6 and BALB/c strains. The mean values of γ -H2AX foci per cell in BALB/c strains are approximately 3.2 fold higher than for the C57BL/6 stains.

In Figure 9, the mean number of foci per cell are displayed as box plots. The *Prkdc* genotype of each fibroblast strain is included in this Figure. It is immediately obvious that the strains with the wild-type *Prkdc* genotypes have the fewest foci/cell and seem to cluster as a distinct group. The cell strains with the *Prkdc*^{BALB} allele appear to fall into two groups as described above. One group includes the BALB/c progenitor strain and has the highest numbers of foci/cell and the other is intermediate between BALB/c and C57BL/6. A one-way analysis

of variance of the 15 strains confirmed that not all the means are equal when alpha is set at 0.05. Further comparisons with Tukey's test indicate that BALB/c is not significantly different from CXB7, 8, 12 or 13 but is different from CXB 9. C57BL/6 is not significantly different from CXB1, 3, 5, or 10; these are the strains with wild-type *Prkdc* genotypes. The remaining strains with intermediate numbers of foci, CXB4, 6, 11 and 2 are not significantly different from one another. These results suggest that the BALB/c allele of *Prkdc* results in inefficient repair on DNA DSB as measured by persistence of γ -H2AX foci. The presence of a group intermediate between BALB/c and C57BL/6, all having the BALB/c *Prkdc* allele, suggests the existence of an unlinked modifier gene. The C57BL/6 allele of that gene would augment DNA DSB repair in cells with the *Prkdc*^{BALB} genotype.

Having examined clonogenic survival and γ -H2AX foci following acute and low dose rate radiation exposures, we next looked at whether the strain distribution patterns of any of these radiobiological endpoints were correlated.

Figure 11-1 displays the relationship between average number of γ -H2AX foci induced by low dose rate ionizing radiation and 50% cell survival under low dose rate ionizing radiation. There is a significant linear relationship between these two endpoints ($p < 0.0001$). Note that the graphs in figure 11 are from Pearson's correlation testing where as the P values we present in the text are from Spearman's rank correlation. The results are essential identical for the two tests. The cell strains appear to fall into three different groups. Group one includes

fibroblasts from CXB7, 8, 9, 12, 13, and BALB/c. They are sensitive to low dose rate ionizing radiation as measured by higher numbers of γ -H2AX foci/cell and a lower total doses required to reduce clonogenic survival to 50%. Group two includes fibroblasts from CXB1, 3, 5, 10 and C57BL/6. Compared to group 1, these strains are resistant to low dose rate ionizing radiation as evidenced by fewer (1/3) γ -H2AX foci/cell average and a higher total dose required to reduce clonogenic survival to 50%. Group three includes fibroblasts derived from CXB2, 4, 6 and 11 and is intermediate in sensitivity to low dose rate ionizing irradiation when compared to groups 1 and 2.

Figure 11-2 displays the relationship between the average number of γ -H2AX foci induced by low dose rate ionizing radiation and average number of γ -H2AX foci induced by acute dose rate ionizing radiation. The two endpoints are not significantly correlated ($p= 0.4505$).

Figure 11-3 displays the relationship between average number of γ -H2AX foci induced by low dose rate ionizing radiation and D0 of cell strains under acute dose ionizing radiation. These two endpoints are not significantly correlated ($p= 0.0845$). Visual inspection of figure 11-3 reveals one strain, CXB9, that appears to be an outlier. If this strain is not included in the analysis low dose rate γ -H2AX foci and D0 are significantly correlated.

Figure 11-4 displays the relationship between average number of γ -H2AX foci induced by high dose rate ionizing radiation and the D0. These two endpoints are significantly correlated ($p= 0.0172$).

Figure 11-5 displays the relationship between average number of γ -H2AX foci induced by high dose rate ionizing radiation and 50% cell survival under low dose rate ionizing radiation. The correlation is not significant ($p= 0.1073$).

Figure 11-6 shows the relationship between 50% cell survival under low dose rate ionizing radiation and D0 of cell strains under acute dose ionizing radiation.

These endpoints are correlated.

One advantage of using RI strains is that the results obtained are cumulative and can be compared between different laboratories. Unpublished G2 chromosomal aberration data are available for the CXB fibroblasts and were generously by H. Nagasawa and A. Roby. Examples of the types of aberrations scored are provided in photomicrographs in Figure 10. The data are summarized in Table 4. Correlating the various G2 aberration endpoints with the ones we have determined yields additional correlations. These are displayed graphically in Figure 11-7 to 11-36.

In addition to being able to correlate radiobiological endpoints with one another, we can also determine if the *Prkdc* genotype is associated with the various endpoints. T tests were run to determine if the endpoints described above are correlated with the *Prkdc* genotypes of the CXB RI strains. Some endpoints like γ -H2AX foci under low dose rate irradiation and low dose rate 50% survival are significantly different ($P<0.05$) between strains with the common and variant alleles of *Prkdc*. Others, such as D0, acute dose rate γ -H2AX foci and G2 chromosome analysis (including chromatid breaks, chromatid exchanges,

chromosome breaks, gaps, and total chromosomal aberration per cell) are not correlated with *Prkdc* genotype. The interactions between the endpoints are summarized diagrammatically in Figure 12.

Table 1 D0 and γ -H2AX foci – Acute Exposures

Strain	1	2	3	4	5	6	7	8	9	10	11	12	13	14	15
D0 (Gy)	1.8	1.9	1.6	1.2	1.8	1.5	0.9	1.1	2.6	2.0	1.6	0.9	1.5	0.9	2.3
γ -H2AX foci	35.31	27.95	32.23	30.60	35.03	36.70	37.21	44.33	32.23	26.39	26.74	32.90	24.67	41.68	27.45

Table 2 50% Survival and γ -H2AX Foci – Low Dose Rate Exposures

Strain	1	2	3	4	5	6	7	8	9	10	11	12	13	14	15
50% (cGy/hr)	2.52	2.01	2.67	1.89	2.61	1.91	1.56	1.63	1.69	2.51	1.97	1.62	1.83	1.68	2.53
γ -H2AX foci	4.50	7.58	5.30	8.86	3.28	8.29	12.59	13.1	14.62	4.46	8.98	11.64	12.82	12.37	4.87

Table 3 Survival Fraction after 2Gy (SF2) of cell strains under acute dose-rate

Strain	1	2	3	4	5	6	7	8	9	10	11	12	13	BAL B/c	C57B L/6
SF2	0.57	0.37	0.55	0.34	0.55	0.39	0.10	0.20	0.45	0.41	0.30	0.16	0.23	0.17	0.48

Table 4 G2 chromosome aberration assay

Cell Strain	Dose (cGy)	Gaps	Total CA/cell	Chromotid type		
				Break	Exchange	Break
CXB1	50	6	1.08	21	2	4
CXB2	50	3	1.44	8	0	3
CXB3	50	3	0.40	9	0	1
CXB4	50	10	1.20	21	2	7
CXB5	50	4.5	0.80	33	1	6
CXB6	50	13	1.40	28	1	6
CXB7	50	14	1.96	33	5	11
CXB8	50	6	1.00	17	5	3
CXB9	50	6	0.76	18	0	1
CXB10	50	6	0.88	18	0	4
CXB11	50	8	0.88	16	1	5
CXB12	50	14	2.00	38	3	9
CXB13	50	6	0.84	15	0	6
BALB/c	50	9	0.80	17	4	4
C57BL/6	50	6.5	0.68	31	2	1

Table 5 Association of radiobiologic endpoints with *Prkdc* genotype

	Low dose-rate γ -H2AX	Low dose-rate 50% survival	Acute dose-rate D0	Acute dose-rate γ -H2AX	Total CA/cell	Chromotid break	Chromotid exchange	Chromosome break	SF2	Gap
T value	-5.81	10.29	1.89	-0.83	-1.45	0.25	-1.13	-1.52	4.27	-2.06
P value	<0.0001	<0.0001	0.1025	0.3003	0.1417	0.9221	0.1363	0.2301	0.0009	0.0620
Degrees of freedom	13	13	13	13	13	13	13	13	13	13

Table 6 Correlationship of endpoints

	LDR H2A	LDR SURV	D0	H2A	Total CA/cell	tid break	tid exch	tid total	some break	Gaps	SF2
LDR H2A	1	-0.84463	-0.46003	0.21090	0.20572	-0.17563	0.26407	-0.09302	0.09395	0.34433	-0.69348
		<0.0001	0.0845	0.4505	0.4620	0.5313	0.3416	0.7416	0.7391	0.2088	0.0041
LDR SURV		1	0.67926	-0.43253	-0.57603	-0.18100	-0.54281	-0.27013	-0.44628	-0.64129	0.88114
			0.0054	0.1073	0.0246	0.5186	0.0365	0.3302	0.0954	0.0100	<0.0001
D0			1	-0.60343	-0.61387	-0.17617	-0.68095	-0.34654	-0.64183	-0.61692	0.78418
				0.0172	0.0149	0.5286	0.0052	0.2057	0.0099	0.0143	0.0005
H2A				1	0.50134	0.40269	0.75254	0.53626	0.26222	0.42761	-0.27281
					0.0569	0.1367	0.0012	0.0393	0.3451	0.1119	0.3252
Total CA/Cell					1	0.58797	0.57318	0.63172	0.78918	0.76655	-0.49687
						0.0212	0.0255	0.0115	0.0005	0.0009	0.0595
tid_break						1	0.51348	0.96948	0.52314	0.59149	-0.04395
							0.0503	<0.0001	0.0454	0.0202	0.8764
tid_exch							1	0.68708	0.36460	0.63332	-0.52311
								0.0047	0.1815	0.0113	0.0454
tid_total								1	0.54301	0.63879	-0.16473
									0.0365	0.0104	0.5574
some break									1	0.64979	-0.52987
										0.0087	0.0422
Gaps										1	-0.62637
											0.0125
SF2											1

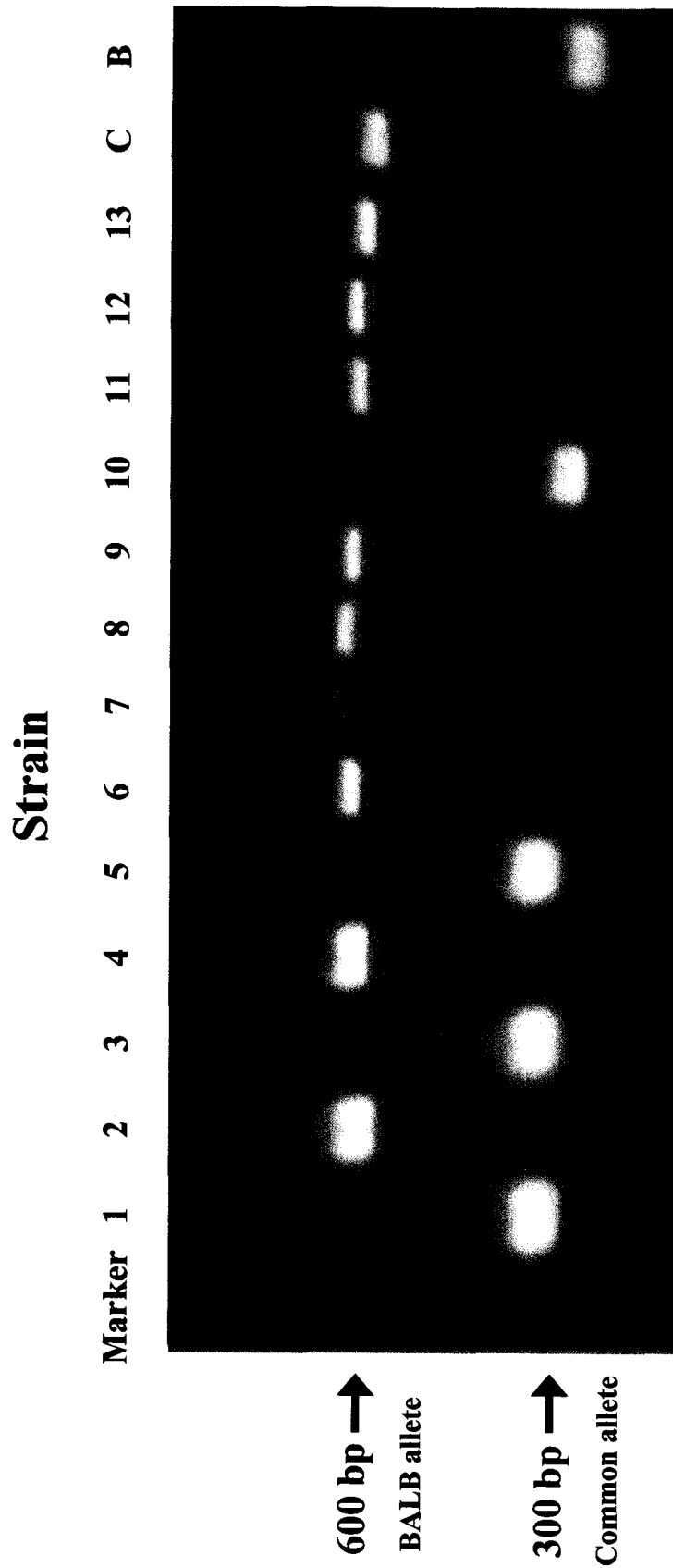


Figure 1 *Prkdc* polymorphism in CXB fibroblasts samples are indicated by line number (e.g. 1 = CXB1). C is BALB/c and B is C57BL/6

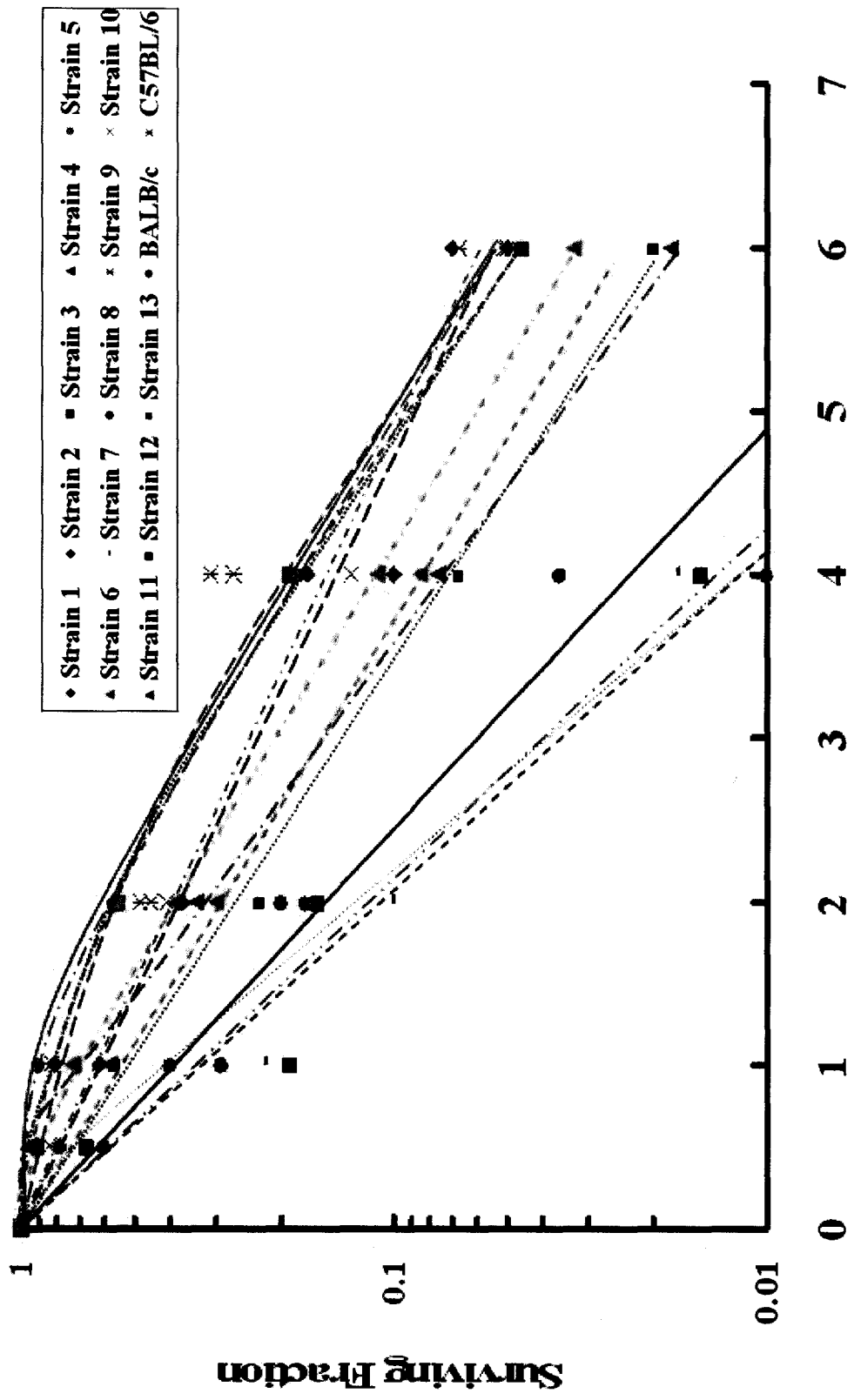
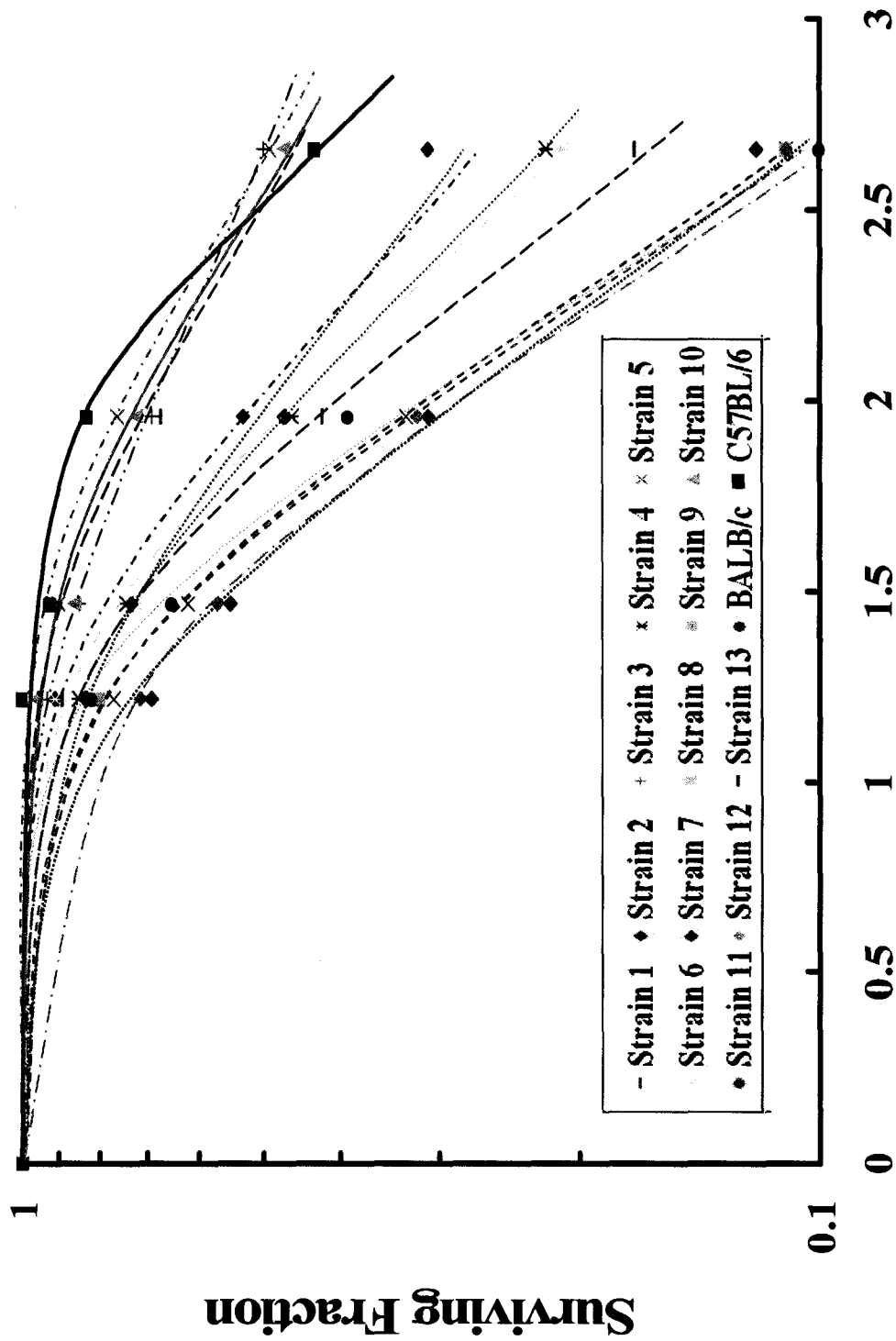


Figure 2 surviving fraction after acute dose irradiation



Dose Rate (cGy/hour)

Figure 3 cell strains surviving fraction after low dose-rate irradiation

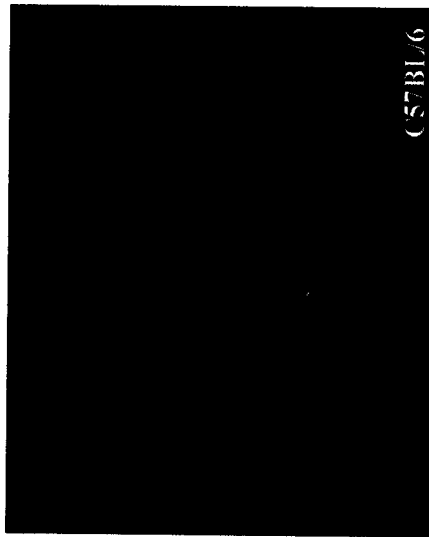
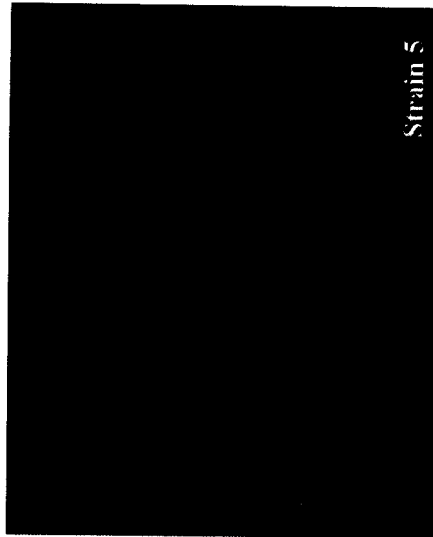
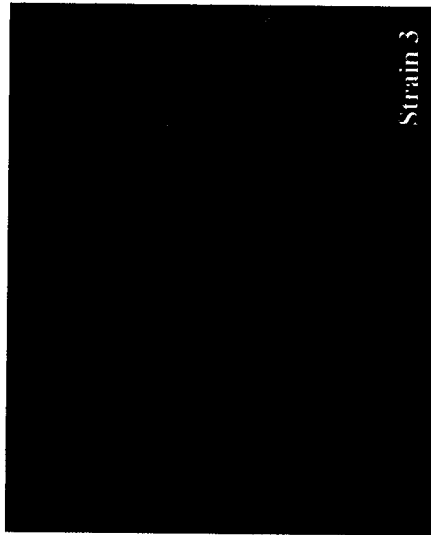
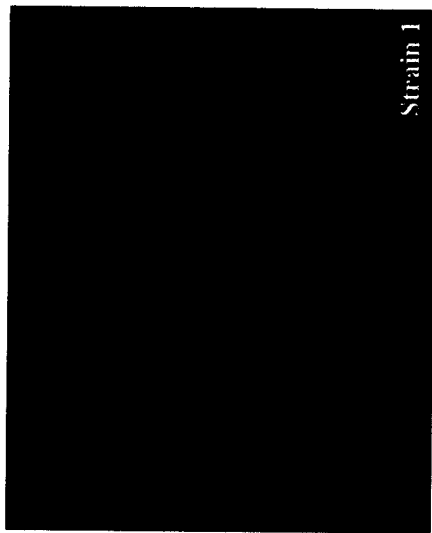


Figure 4a γ -H2AX foci in cell strains after acute dose irradiation

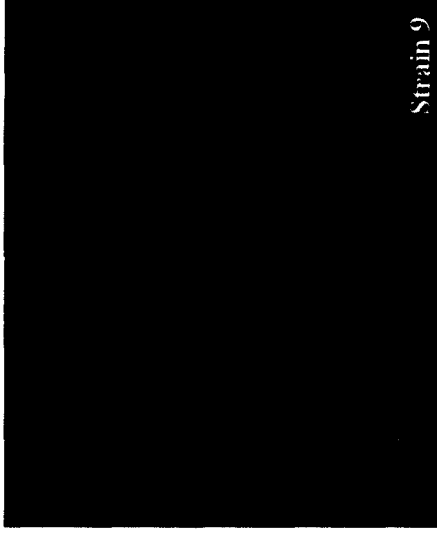
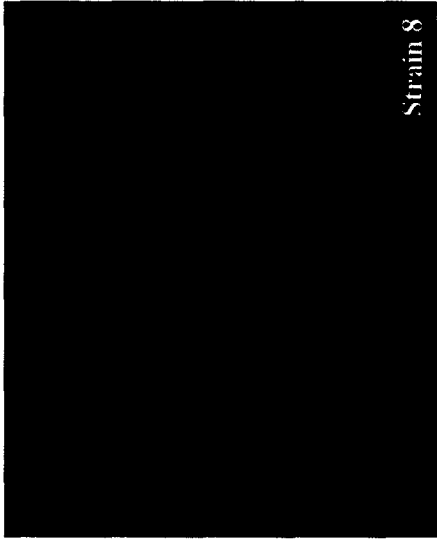
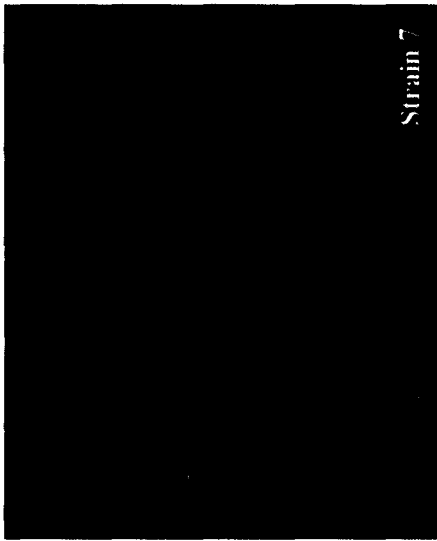


Figure 4b γ -H2AX foci in cell strains after acute dose irradiation

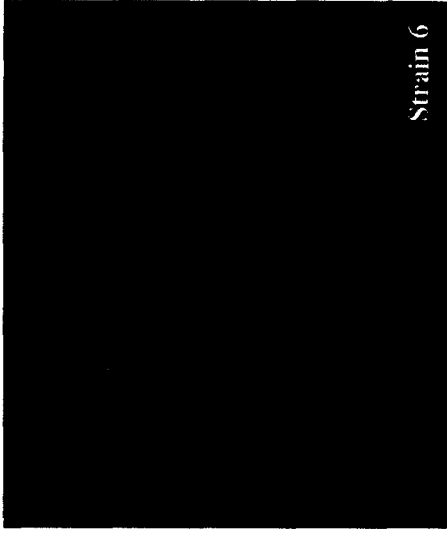
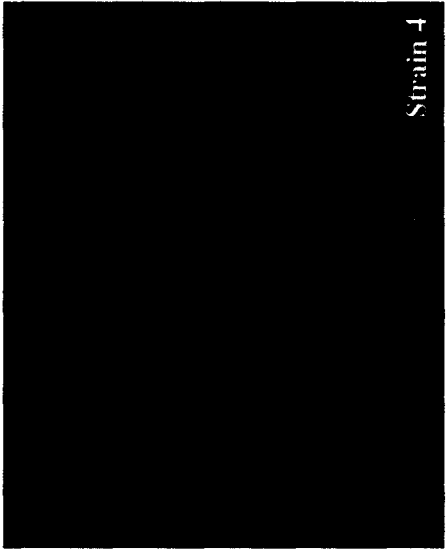
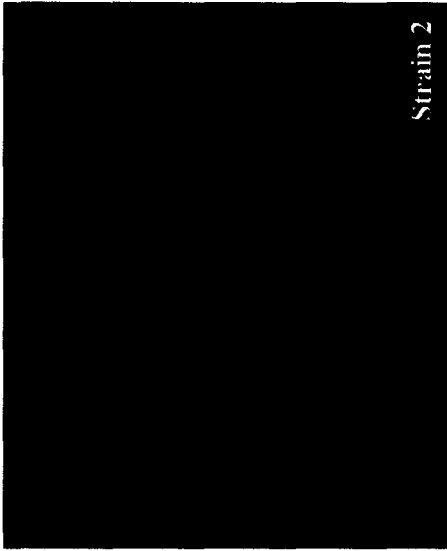


Figure 4c γ -H2AX foci in cell strains after acute dose irradiation

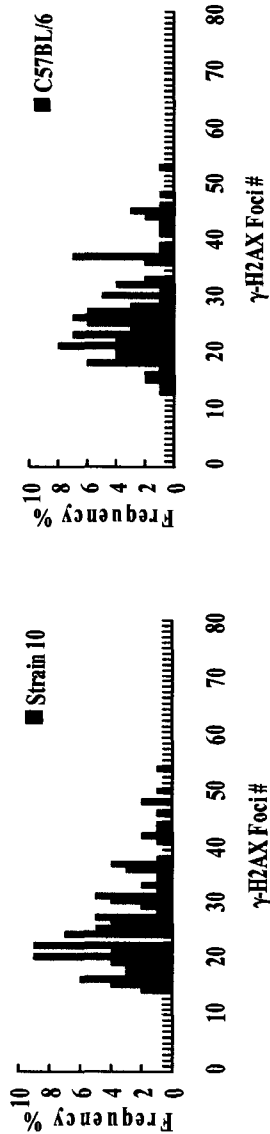
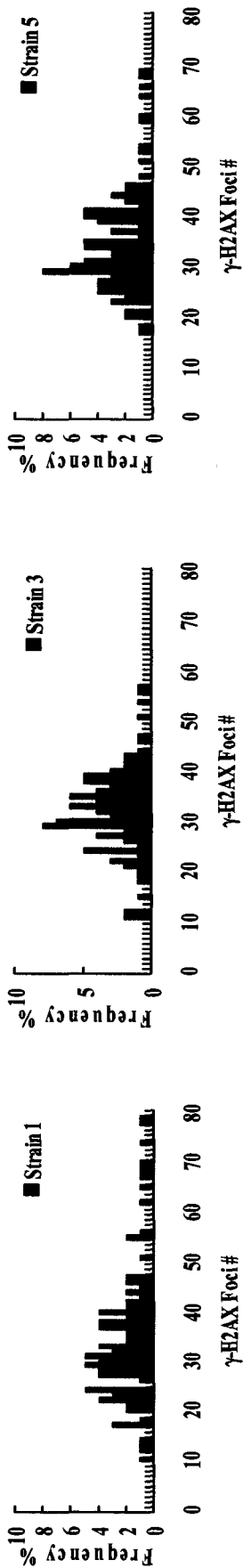


Figure 5a distribution of γ -H2AX foci in cell strains after acute dose irradiation

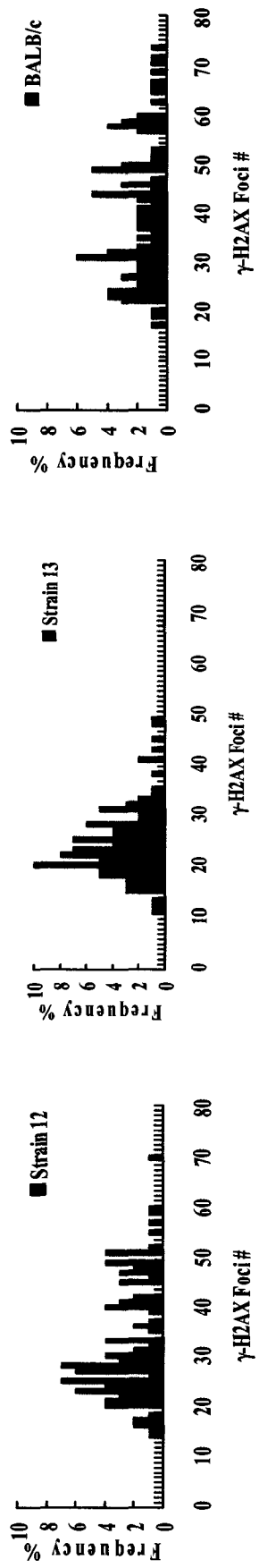
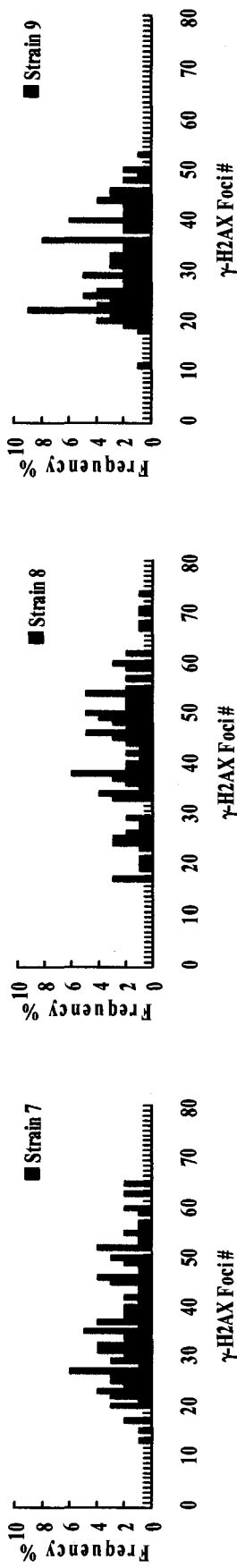


Figure 5b distribution of γ -H2AX foci in cell strains after acute dose irradiation

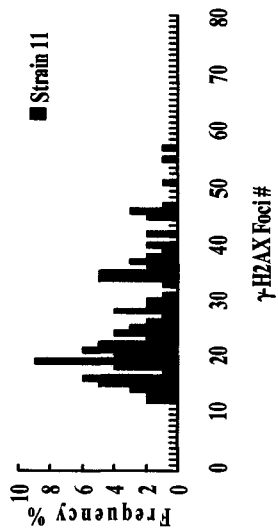
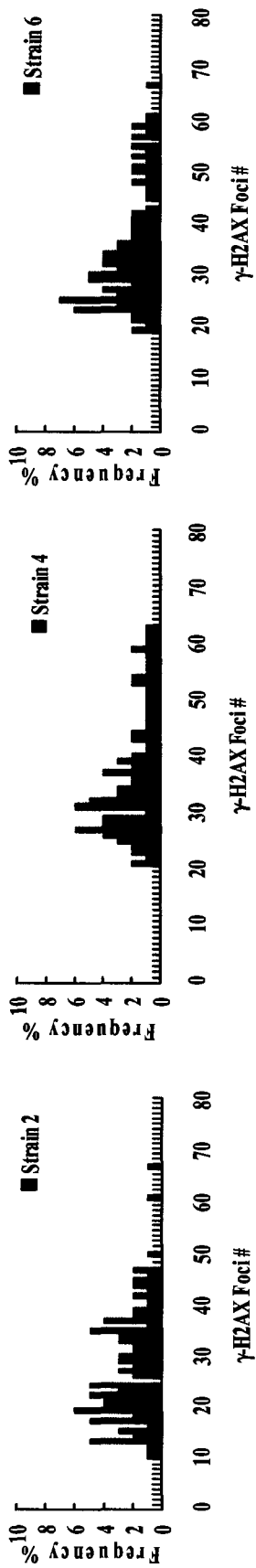


Figure 5c distribution of γ -H2AX foci in cell strains after acute dose irradiation

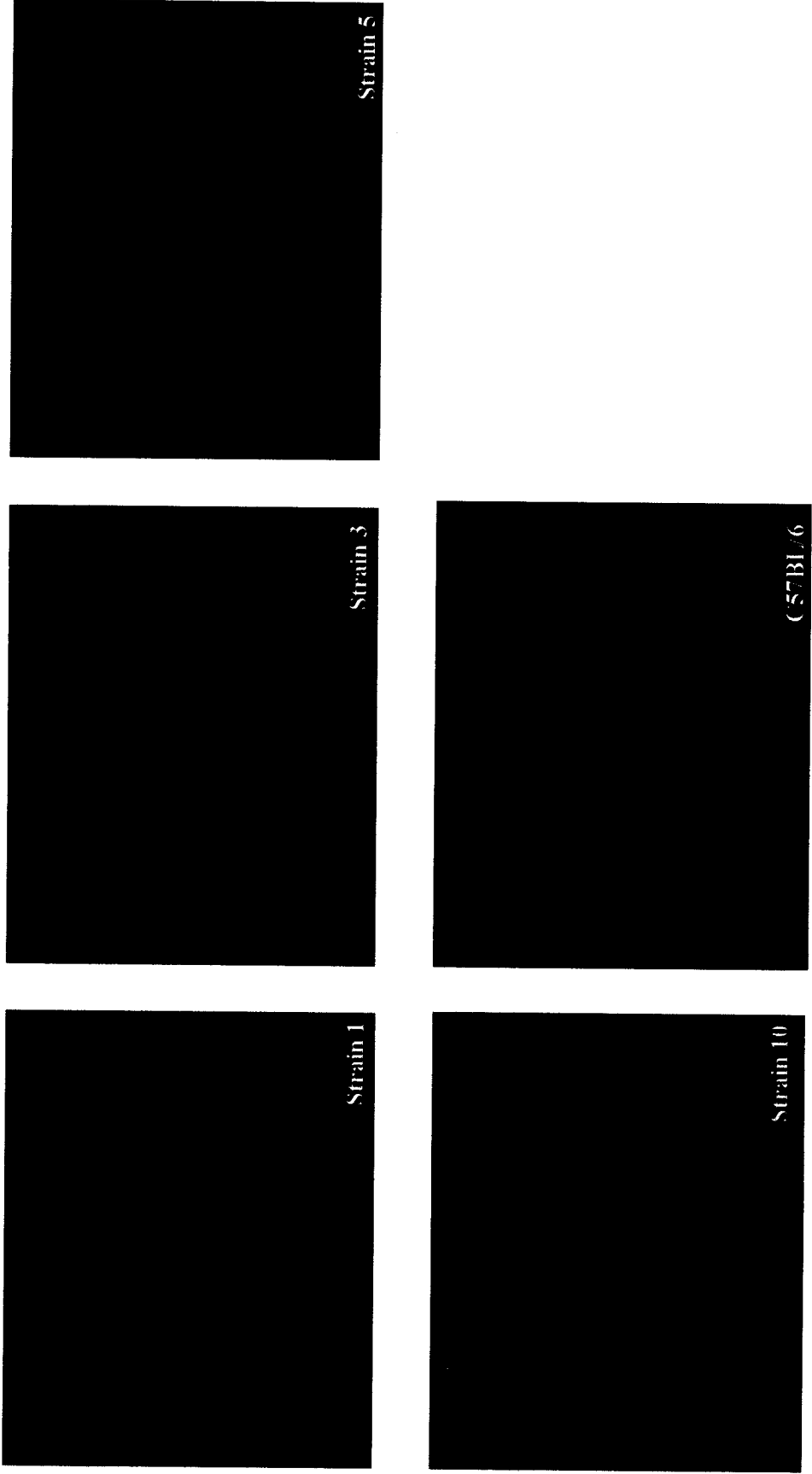


Figure 7a γ -H2AX foci in cell strains after low dose-rate irradiation

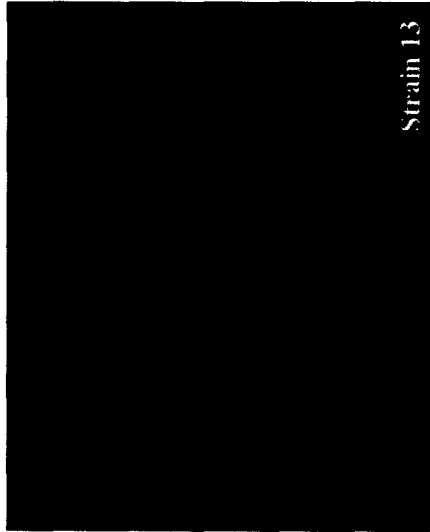
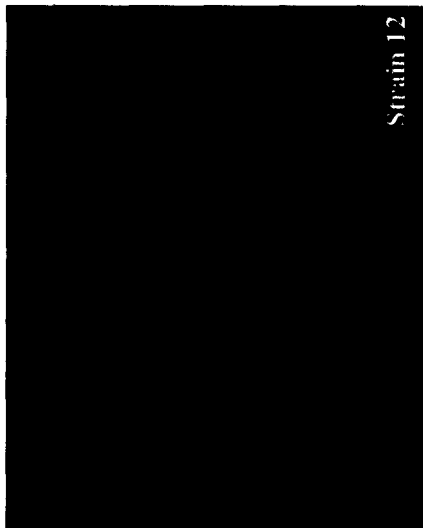
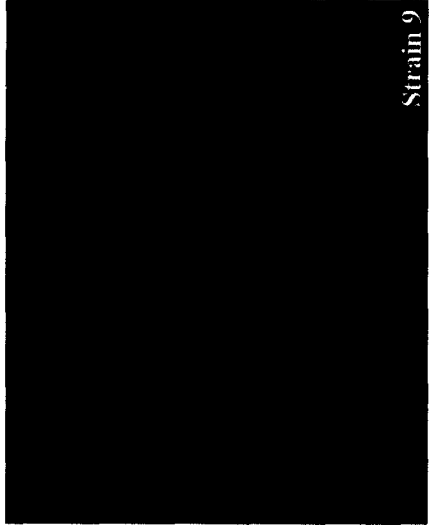
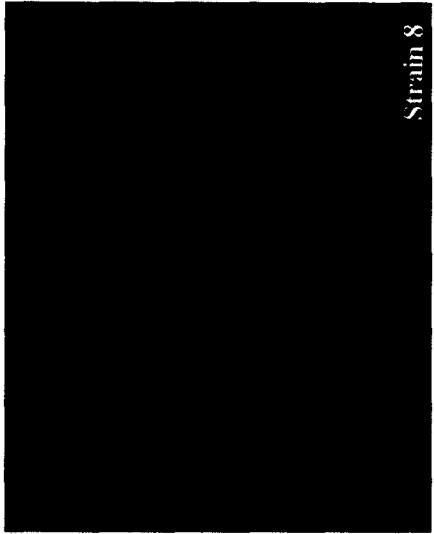
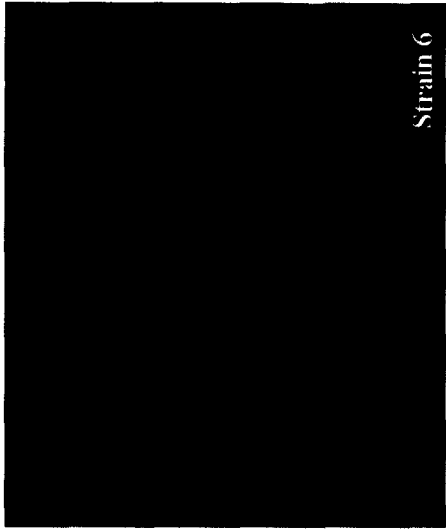


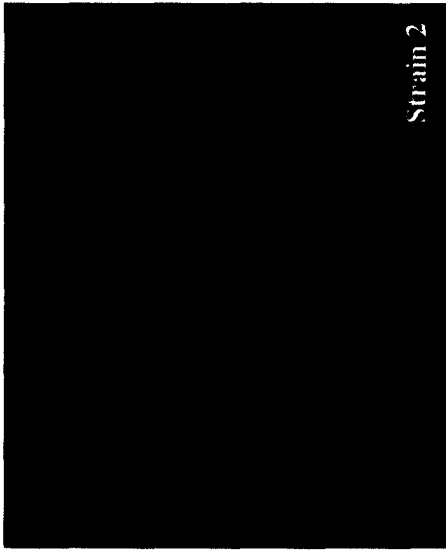
Figure 7b γ -H2AX foci in cell strains after low dose-rate irradiation



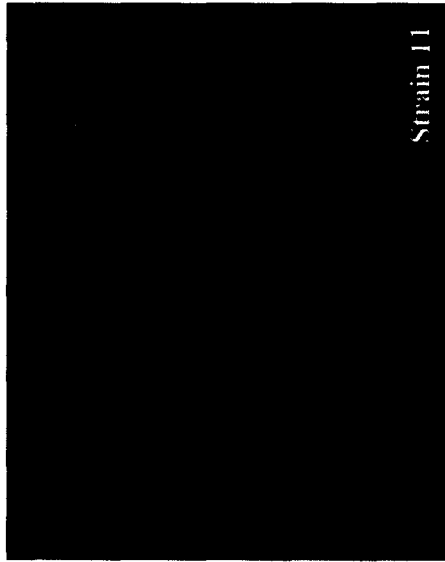
Strain 6



Strain 4



Strain 2



Strain 11

Figure 7c γ -H2AX foci in cell strains after low dose-rate irradiation

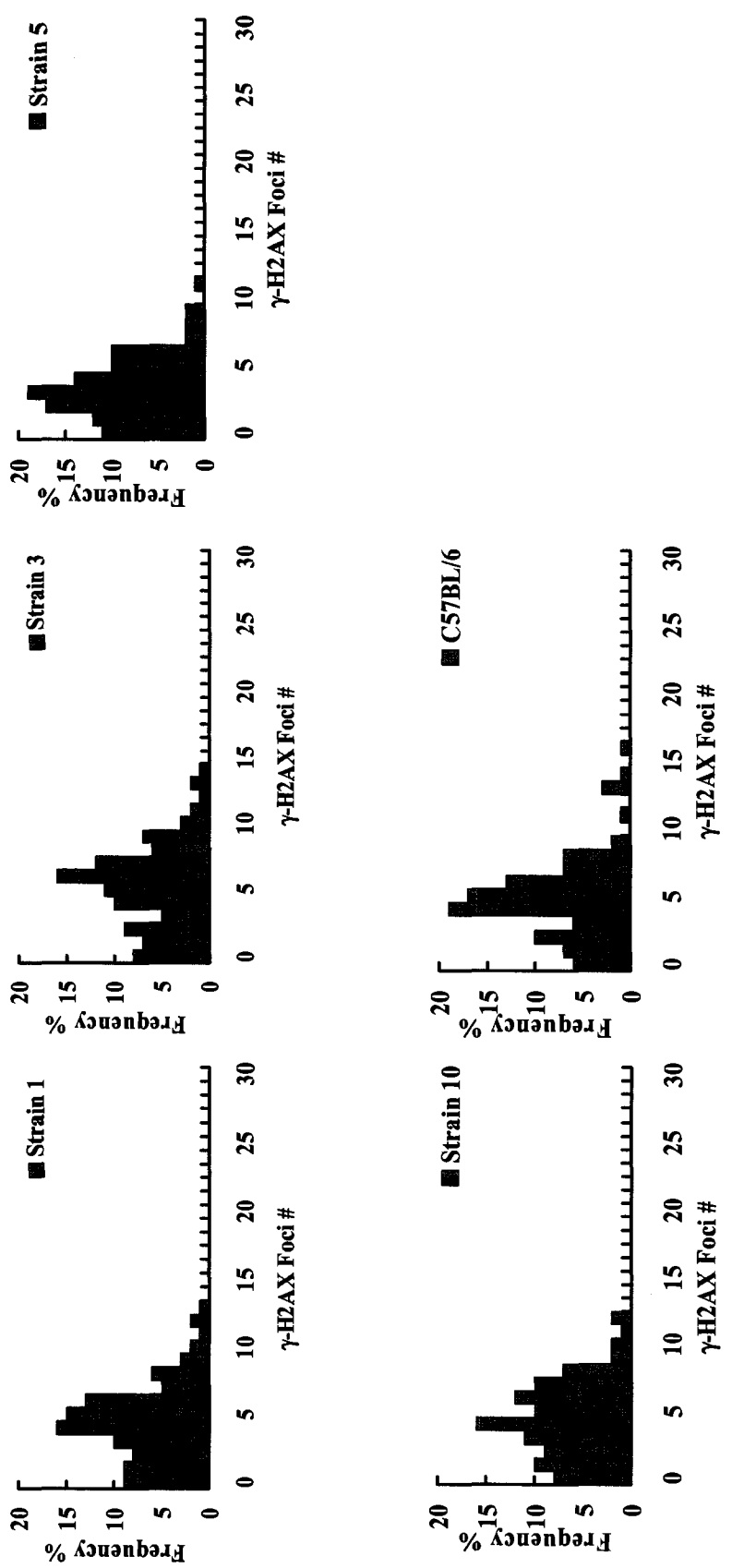


Figure 8a distribution of γ -H2AX foci in cell strains after low dose-rate irradiation

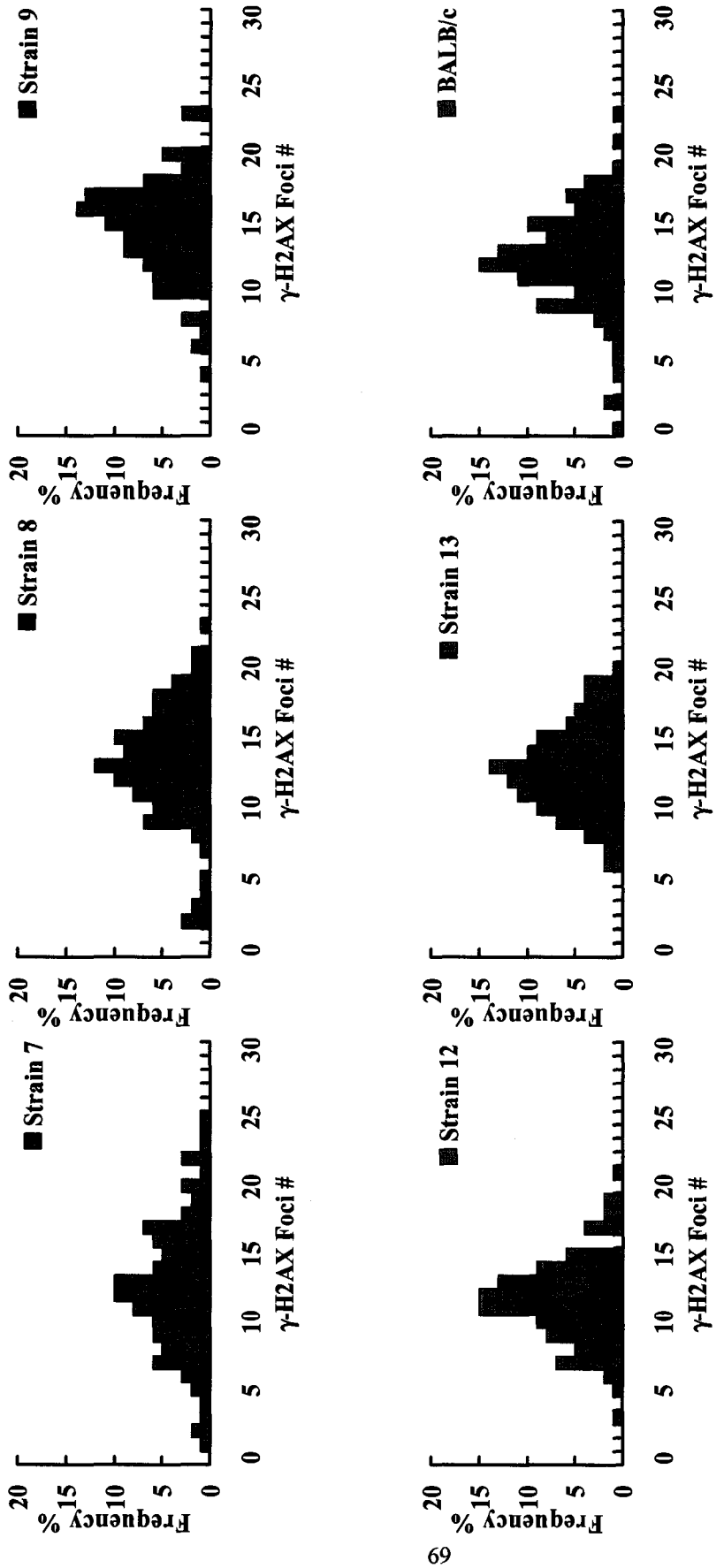


Figure 8b distribution of γ -H2AX foci in cell strains after low dose-rate irradiation

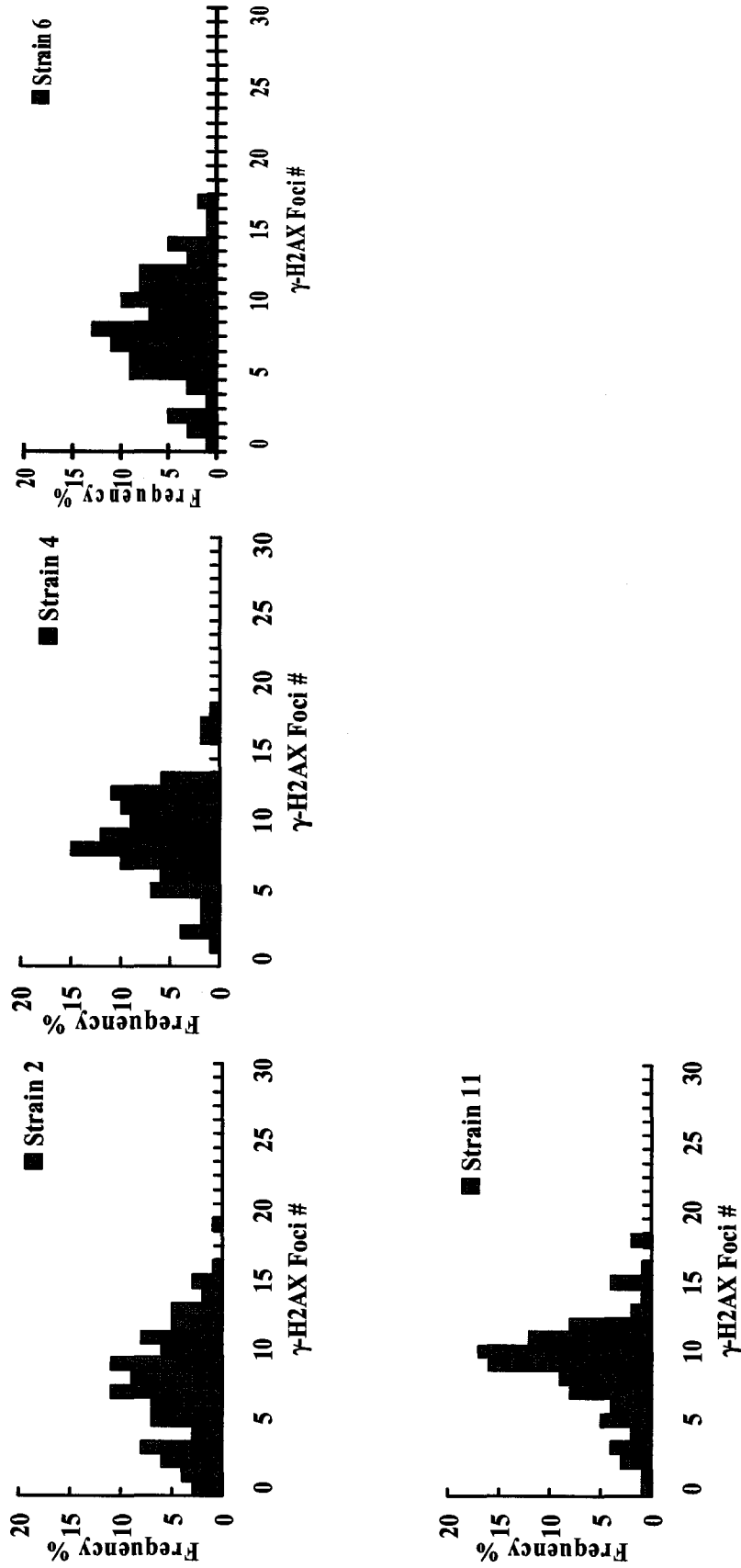


Figure 8c distribution of γ -H2AX foci in cell strains after low dose-rate irradiation

Low dose rate γ -H2AX Foci

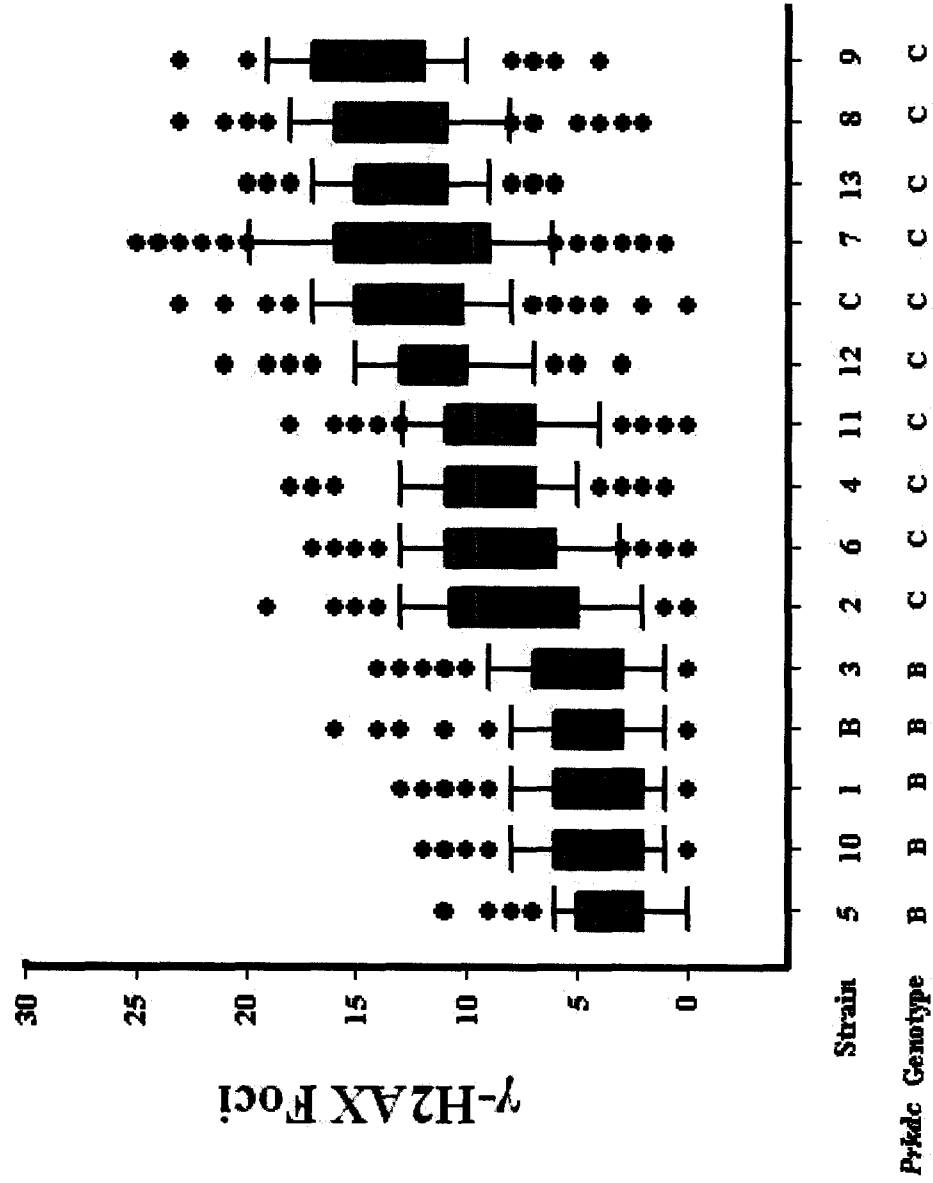


Figure 9 distribution of γ -H2AX foci after low dose-rate irradiation plot
box analysis

E = Exchange



G = Gap

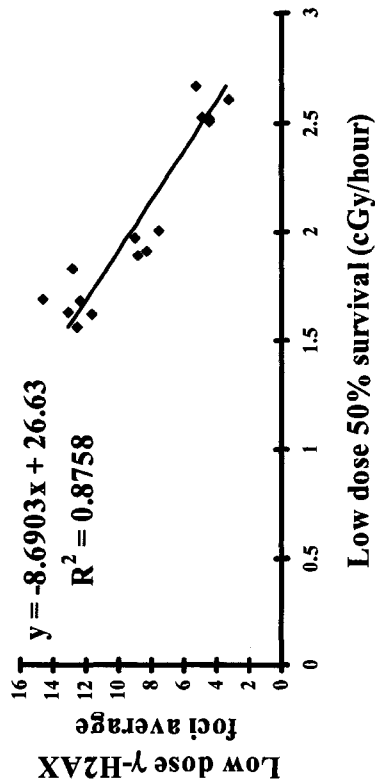


B = Break

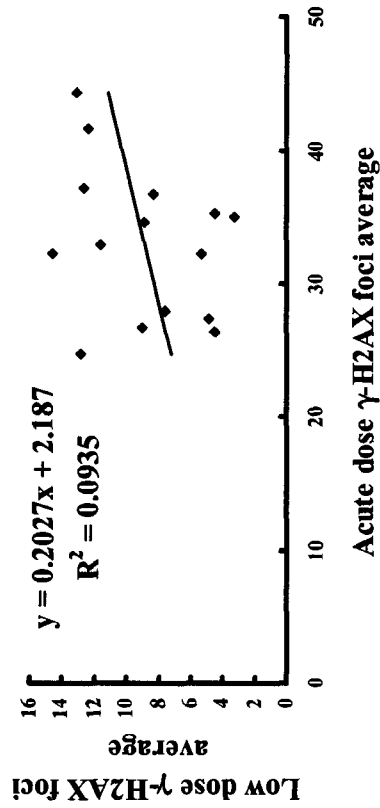


Figure 10 G2 Chromosome aberration analysis, examples of cytogenetic aberrations

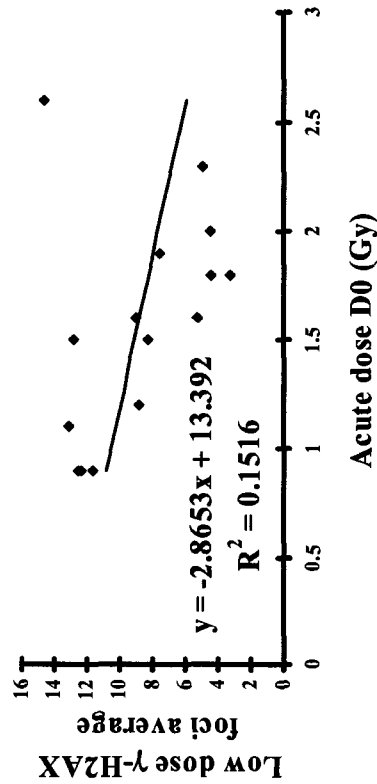
Low dose γ -H2AX foci average VS. Low dose 50% survival



Low dose γ -H2AX foci average VS. Acute dose γ -H2AX foci average



Low dose γ -H2AX foci average VS. Acute dose D0



Acute dose γ -H2AX foci average VS. Acute dose D0

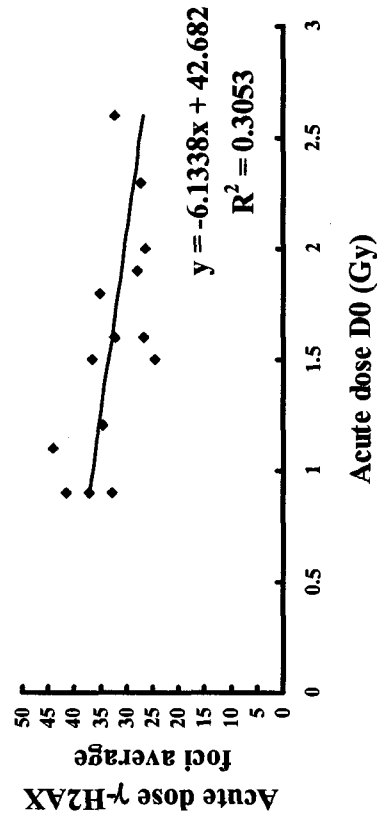
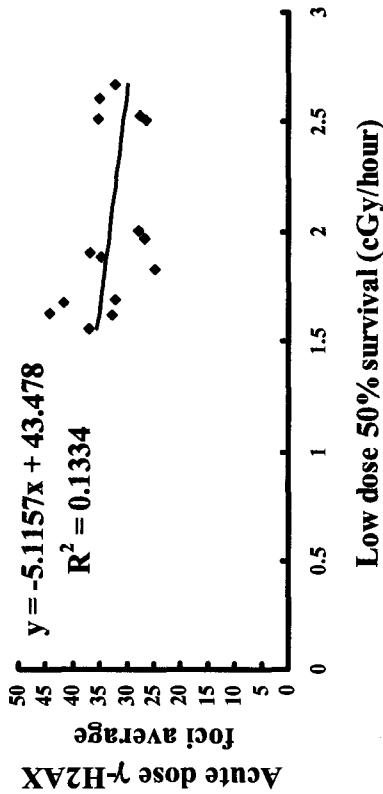
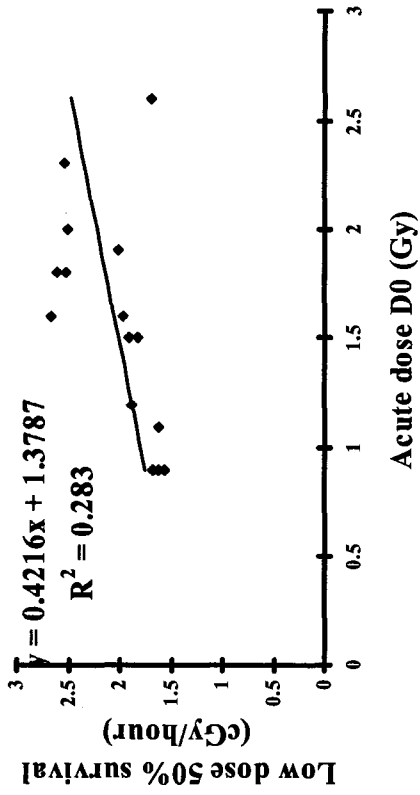


Figure 11 correlations of radiobiologic endpoints in CXB fibroblast strains

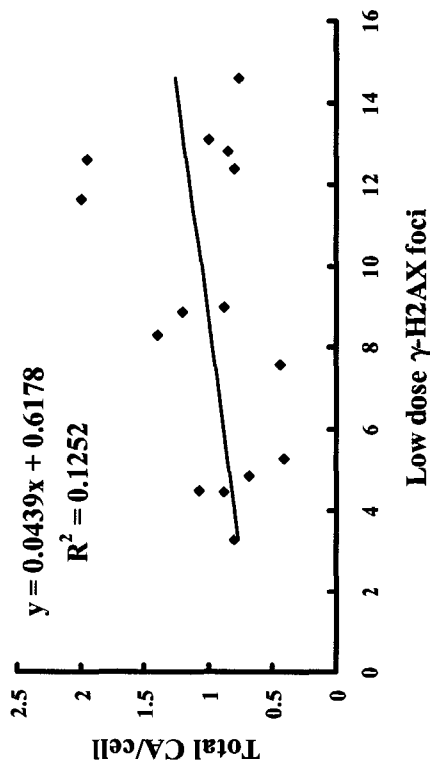
Acute dose γ -H2AX foci average VS. Low dose 50% survival



Low dose 50% survival VS. Acute dose D0



Total CA/cell VS. Low dose γ -H2AX foci



Gaps VS low dose γ -H2AX foci average

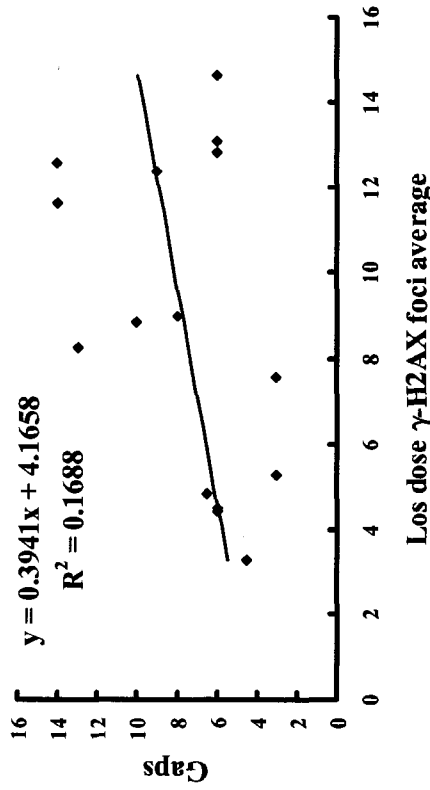
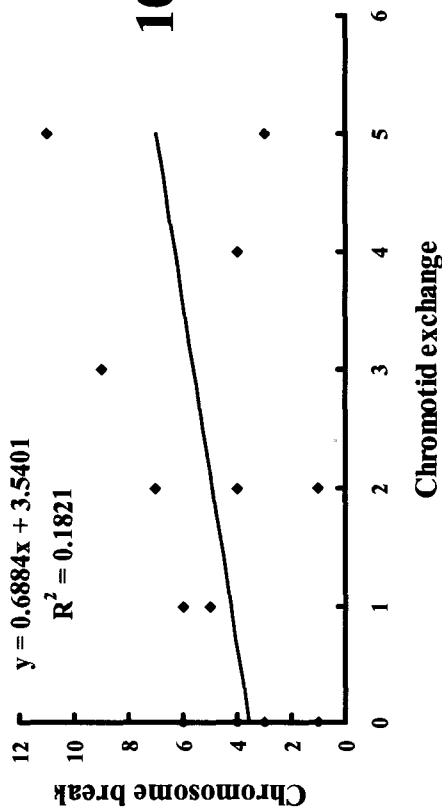
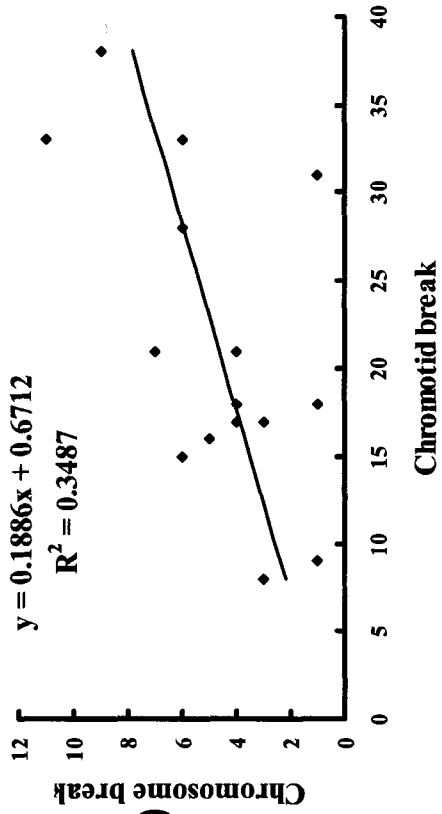


Figure 11 continued

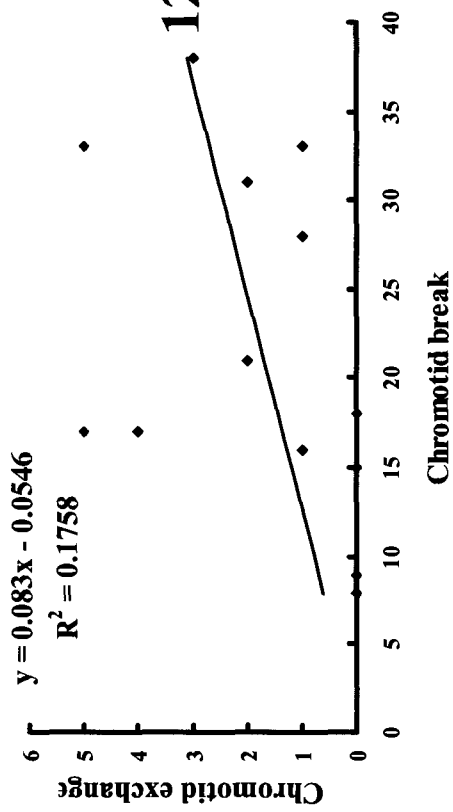
Chromosome break VS. Chromotid exchange



Chromosome break VS. Chromotid break



Chromotid exchange VS. Chromotid break



Chromosome break VS. Total CA/cell

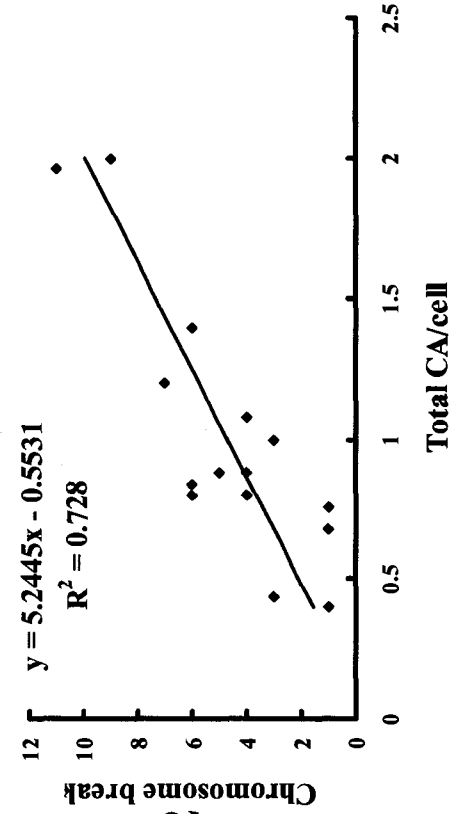
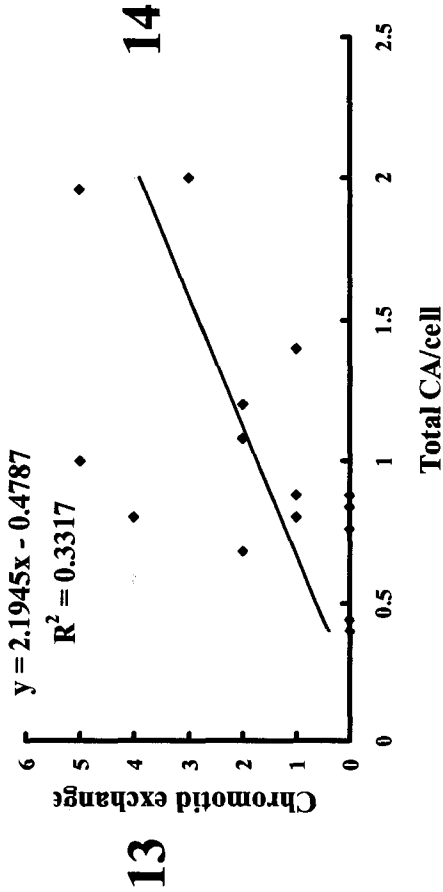
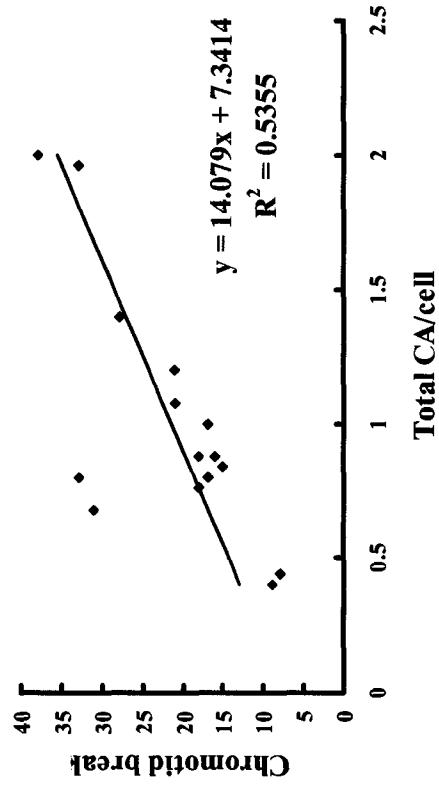


Figure 11 continued

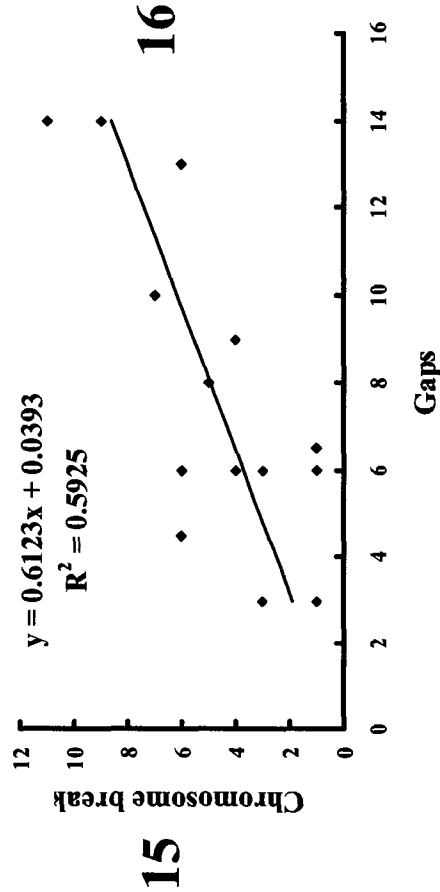
Chromatid exchange VS. Total CA/cell



Chromatid break VS. Total CA/cell



Chromosome break VS. Gaps



Chromatid exchange VS. Gaps

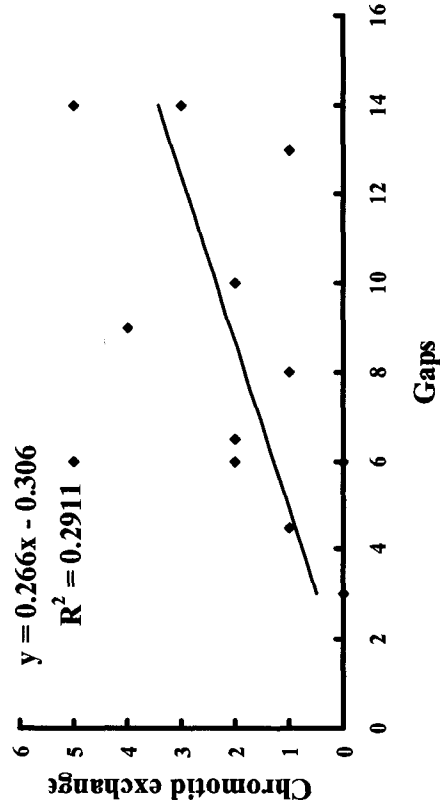
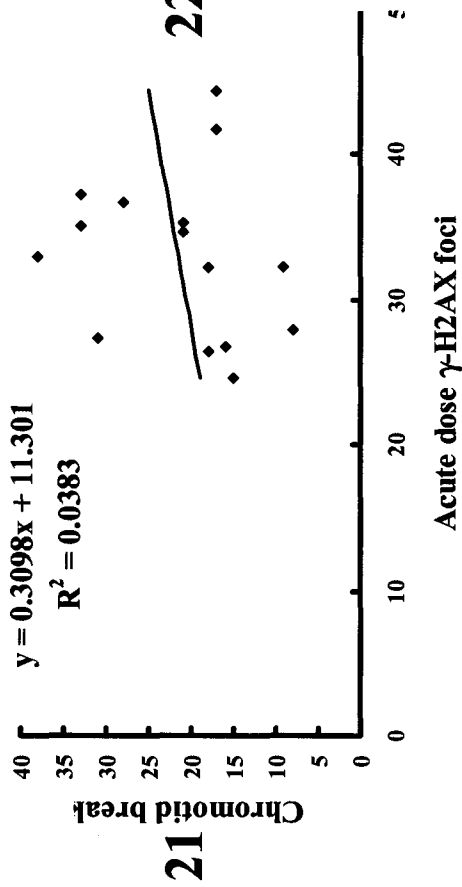
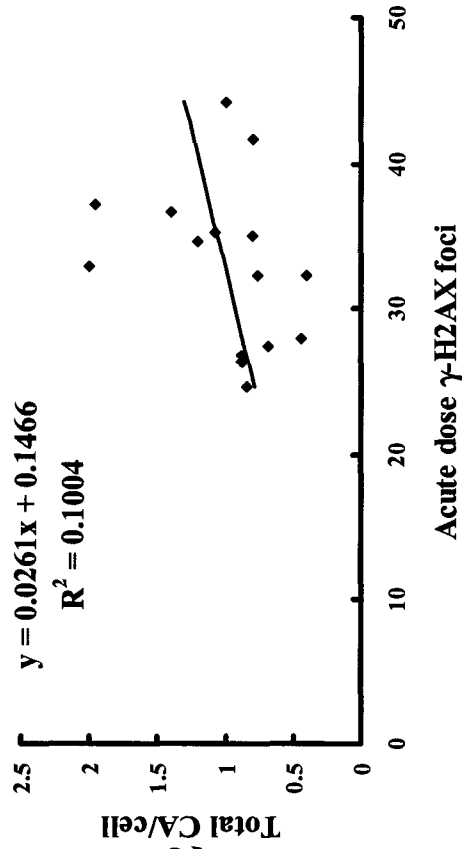


Figure 11 continued

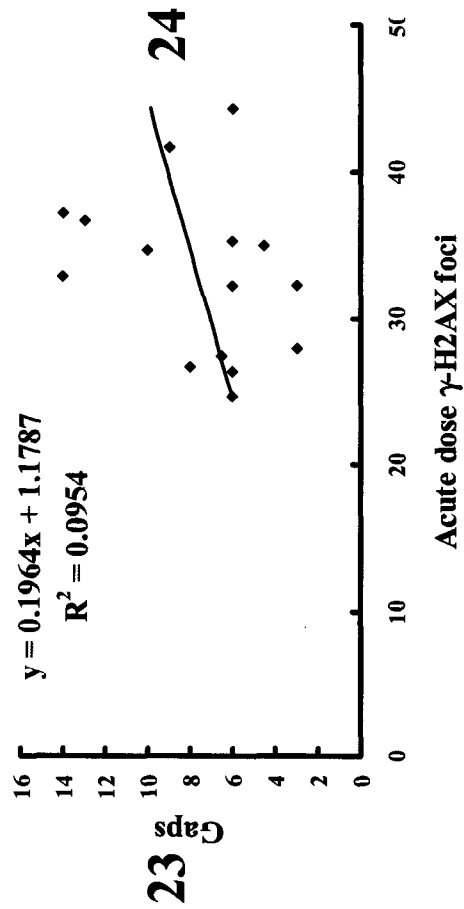
Chromotid break VS. Acute dose γ -H2AX foci



Total CA/cell VS. Acute dose γ -H2AX foci



Gaps VS. Acute dose γ -H2AX foci



Chromosome break VS. Acute dose D0

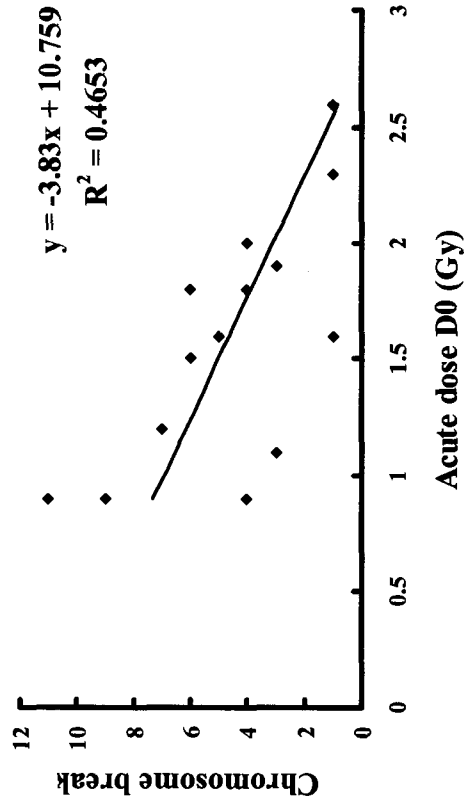


Figure 11 continued

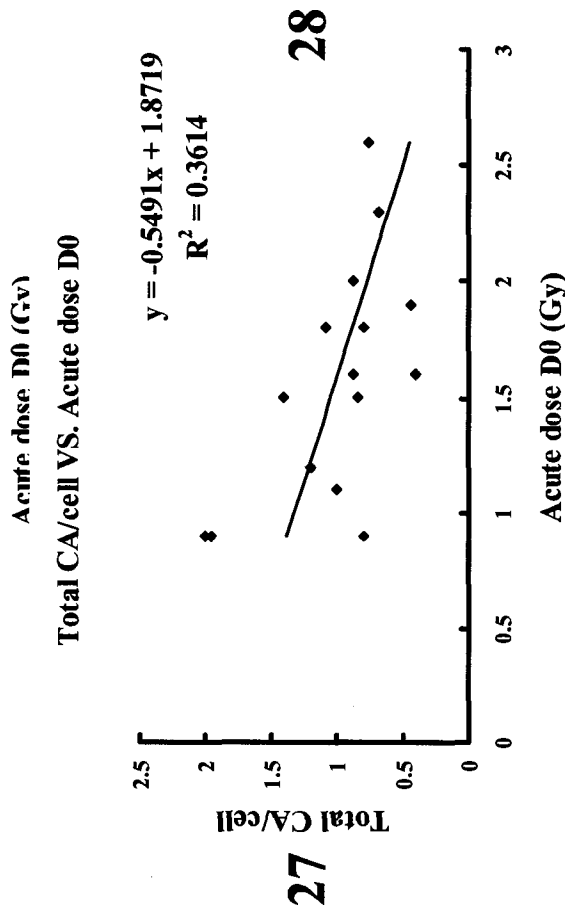
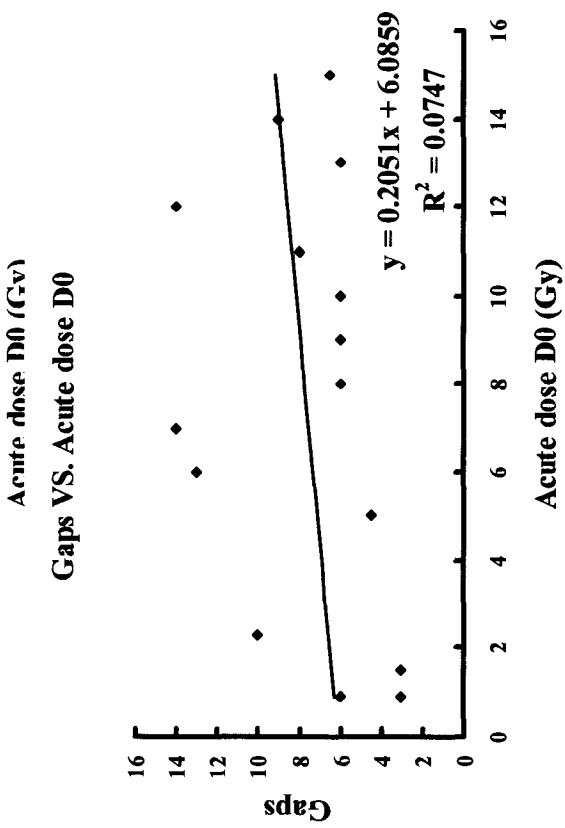
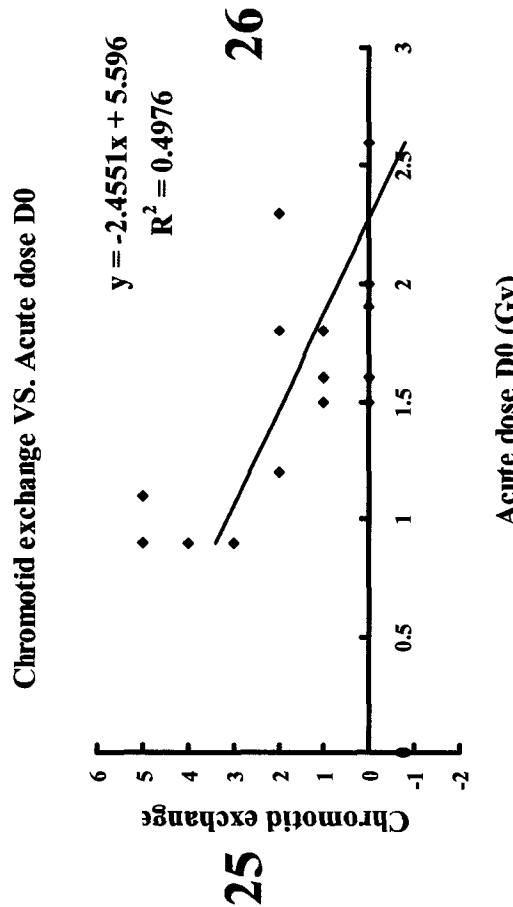
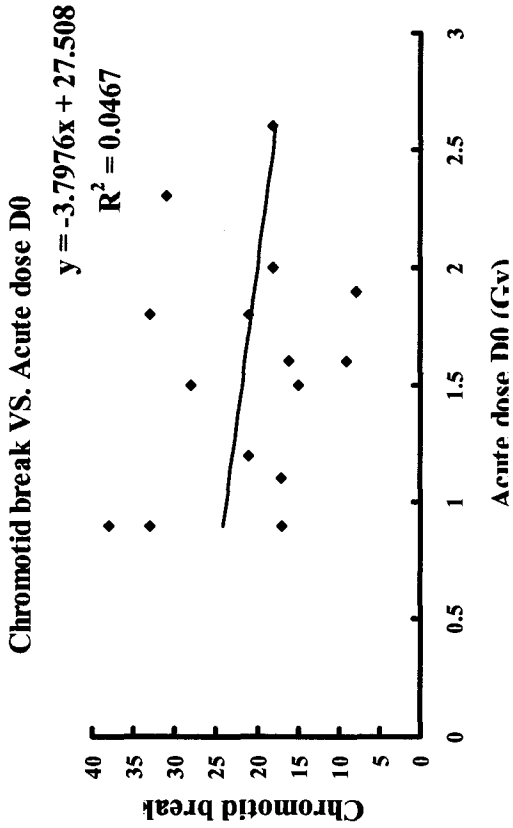


Figure 11 continued

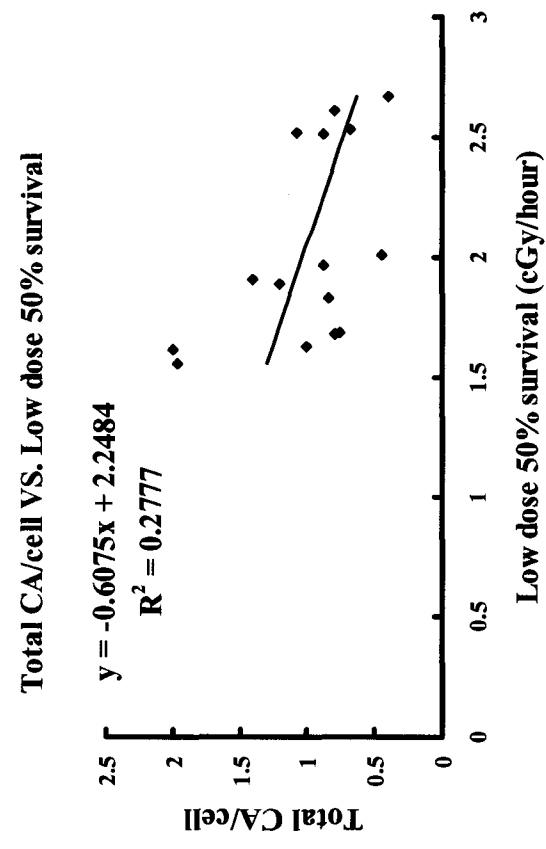
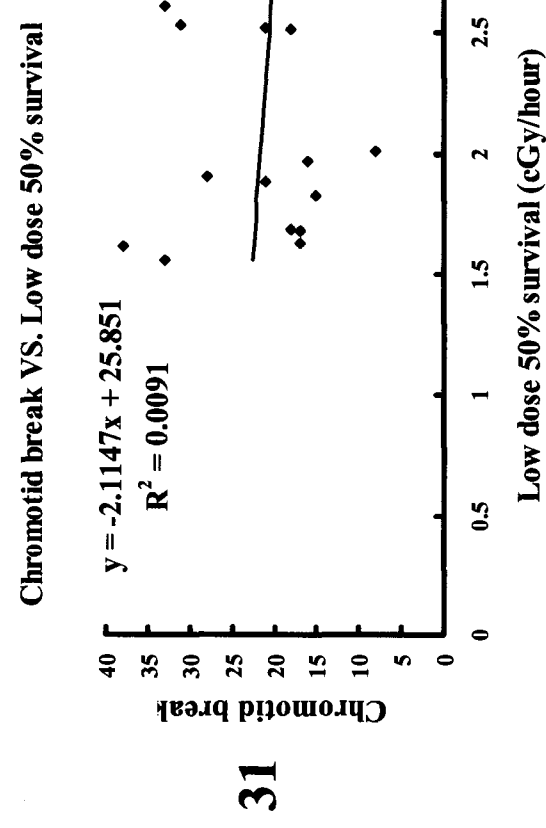
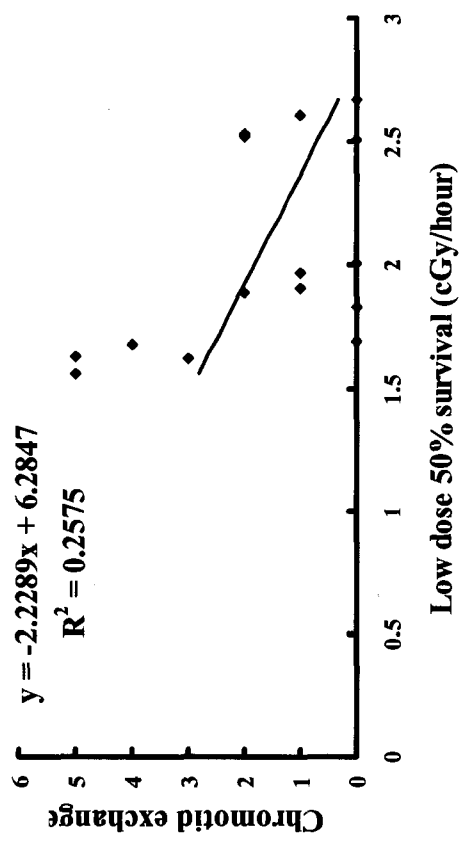
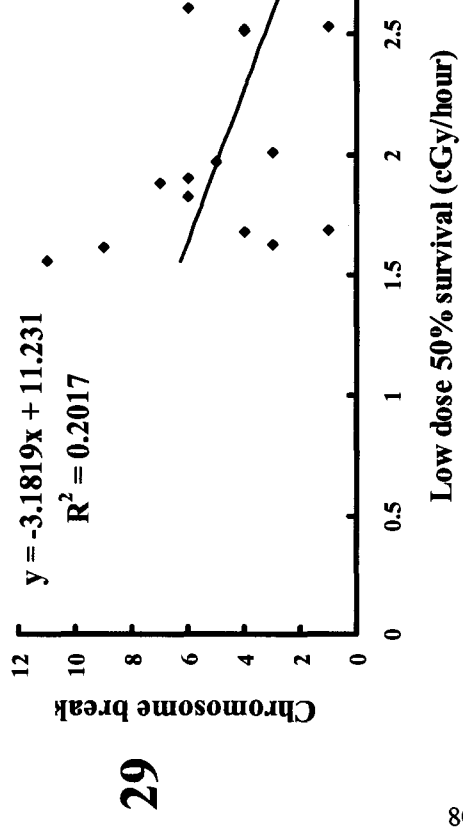
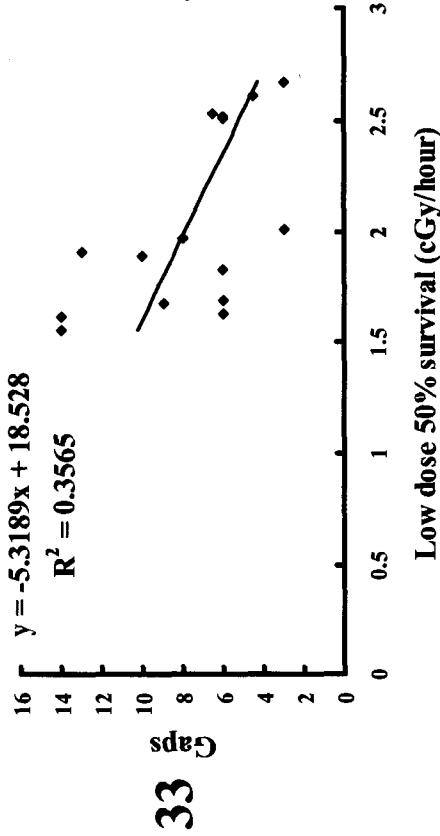
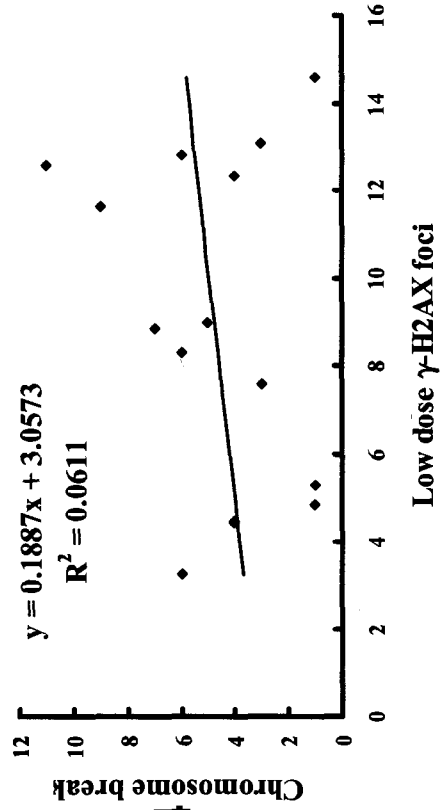


Figure 11 continued

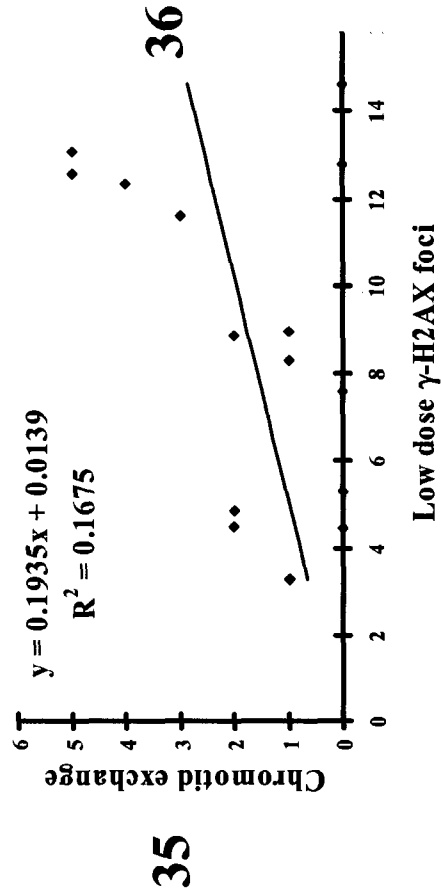
Gaps VS. Low dose 50% survival



Chromosome break VS. Low dose γ -H2AX foci



Chromatid exchange VS. Low dose γ -H2AX foci



Chromatid break VS. Low dose γ -H2AX foci

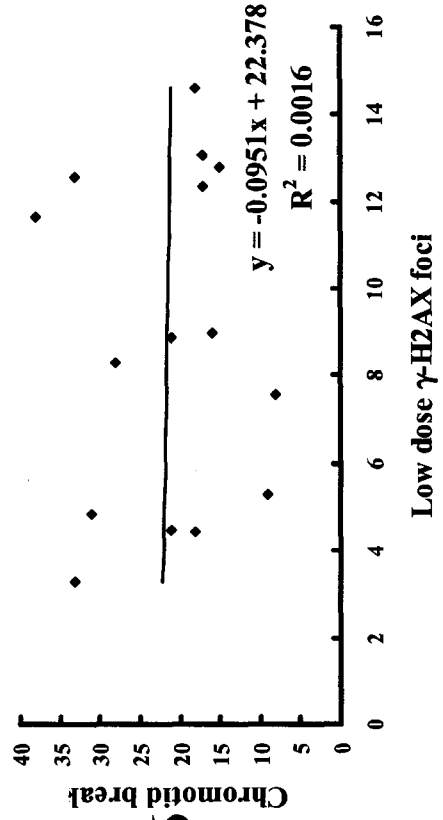


Figure 11 continued

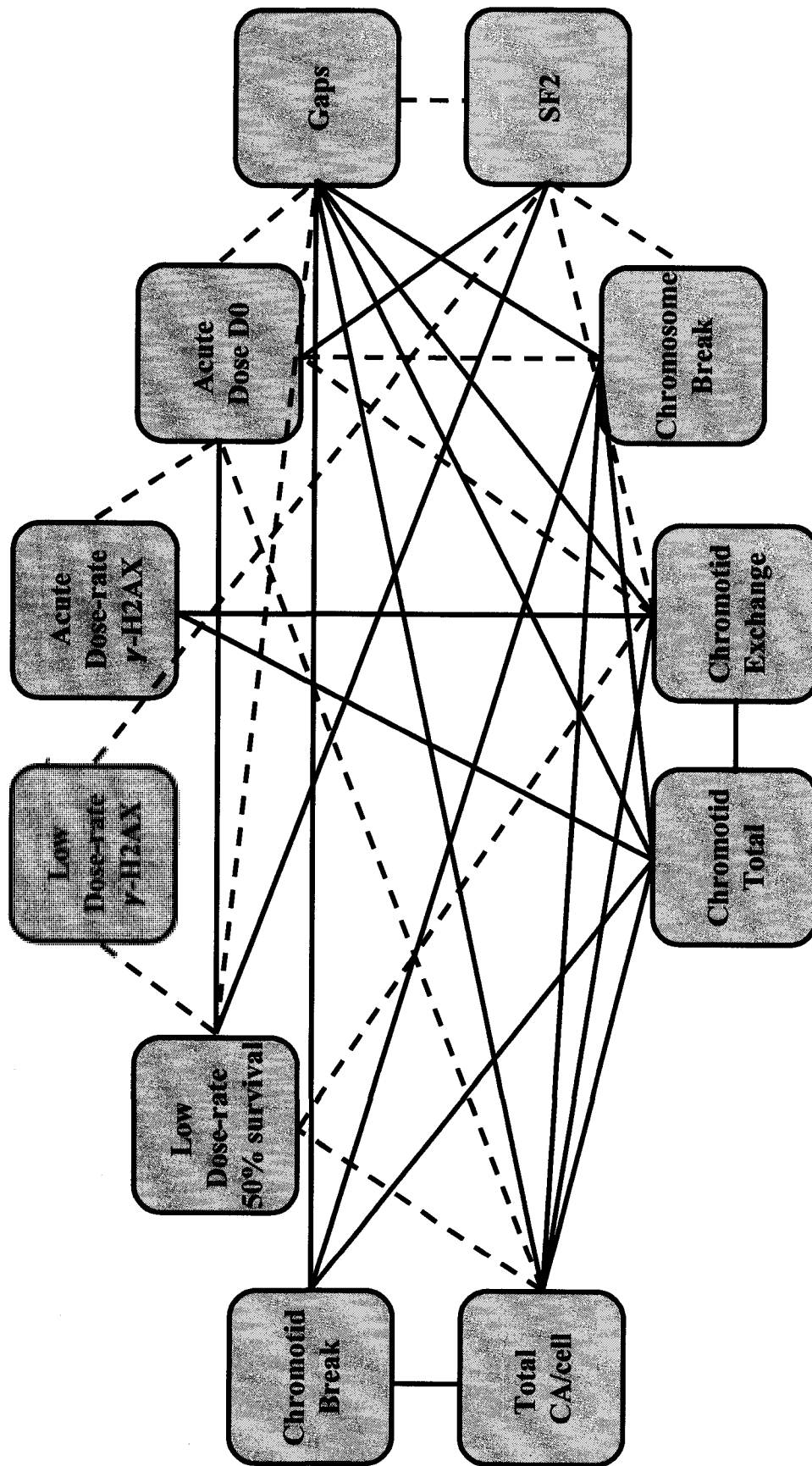


Figure 12 Interactions between traits in CXB RI strains. Solid lines indicate positive correlations. Dashed lines indicate negative correlations.

Discussion

We have identified several radiobiological endpoints that differ between C57BL/6 and BALB/c mice. Treating these endpoints as phenotypic traits we find that they segregate in RI strains in the CXB panel. For the most part the progenitor strains are among those with the highest and lowest values of the traits assayed. Consequently, if any of the traits are under multigenic control all the polymorphisms with major effects that increase the trait value are in one strain and all that decrease it are in the other.

There is a positive correlation between clonogenic survival at low dose rate (LDR) exposures and acute exposures which is not surprising. The correlation is better (R is greater) for LDR survival and SF2 than for LDR and D0. Low dose rate survival is thought to be strongly associated with repair capacity. So, the better correlation of LDR survival with SF2 might result from SF2 being more representative of the low dose region of the survival curve than D0 and thus more reflective of repair capacity than D0.

γ -H2AX focus formation at low dose rate does not correlate with focus formation following acute exposures. We are hesitant to draw conclusions from this observation because we only measured γ -H2AX focus formation at a single time point after acute exposure. There is adequate evidence for cell strain differences

in the kinetics of γ -H2AX focus formation and disappearance. Thus, a single time point is probably not a useful metric of this endpoint and additional data will have to be collected before any useful analysis can be done. On the other hand, quantifying γ -H2AX foci at a single time point immediately after prolonged low dose rate irradiation does seem to measure DNA DSB capacity. This may be because a steady state is reached between *de novo* DNA double strand break formation and its repair during protracted exposures.

There is a negative correlation between γ -H2AX foci following low dose rate exposure and survival under low dose rate exposure conditions. That is, fibroblast strains that accumulate the greatest numbers of foci are the least like to survive. This is not surprising; defective repair has been linked low clonogenic survival in other systems. But, there are two interesting and potentially novel aspects to our findings. The first is that that the DNA repair deficit and diminished clonogenic survival in the BALB/c fibroblasts have no overt phenotypic consequences at the level of the whole organism (though, see below) and are probably within the normal physiologic range for mice. This is in distinction to biallelic *ATM* mutations in ataxia-telangiectasia patients or *Prkdc* mutations in SCID mice. The second is that correlation between low dose rate γ -H2AX focus formation and low dose rate survival is not bimodal; that is, there is not a BALB/c-like group and a C57BL/6-like group (Figure 11-1). Rather, there appears to be three groups with the additional one intermediate between the

BALB/c-like group and a C57BL/6-like group. As discussed in the Results Section, all of the RI strains that have low numbers of γ -H2AX foci and high survival have the C57BL/6 allele of *Prkdc*. The RI strains with high numbers of γ -H2AX foci and low survival have the BALB/c allele of *Prkdc* and so do the strains with intermediate numbers of foci and intermediate survival. Given that RI mice are considered homozygous at every locus (in reality there is some small amount of residual heterozygosity), the simplest explanation for these results is that there is an unlinked gene that modifies the effects of *Prkdc*^{BALB}. The C57BL/6 allele of this gene increases low dose rate survival and decreases γ -H2AX foci in fibroblasts from *Prkdc*^{BALB/BALB} mice.

Numbers of γ -H2AX foci following low dose rate exposure are not significantly correlated with clonogenic survival as measured by D0. As noted in the results section, the CXB9 strain seems to be an outlier in the survival results and the correlation is significant if it is omitted from the analysis. Whether the CXB9 results are attributable to experimental error, genetic or epigenetic changes in the cultured fibroblasts, or they reflect the true radiosensitivity of the strain is currently unknown.

There is a negative correlation between γ -H2AX foci following low dose rate exposure and survival as measured by SF2. This finding may have clinical significance. The SF2 assay has potential as a predictor of normal tissue injury in

radiotherapy patients. However, the current assay takes too long to run to have clinical utility. If determining numbers of γ -H2AX foci following low dose rate irradiation can be used in place of determining clonogenic survival after 2 Gy exposures, the time required to complete the assay would be substantially reduced. The other time consuming step in the SF2 assay is the requirement to establish patient fibroblasts *in vitro*. If SF2 correlates with low dose rate γ -H2AX foci in lymphocytes as well as fibroblasts, the need to establish fibroblasts in culture would also be eliminated. This is something that can be investigated using the using the RI strategy that is the basis of this dissertation.

Traits quantified by other research groups using the CXB RI strain panel can be correlated with our results. H. Nagasawa and A. Roby at Colorado State University tested fibroblasts from the CXB RI panel in the G2 chromosomal aberration assay. Several types of chromosome and chromatid aberrations were scored. As expected there is a significant negative correlation between the total chromosome aberrations and survival as measured by D0 and low dose rate clonogenic survival. The SF2 correlation is not quite significant at the $\alpha=0.05$ level.

The correlations between the survival endpoints we measured and G2 chromatid-type aberrations measured by Nagasawa and Roby are interesting and unexpected. Chromatid breaks were not significantly correlated with the

clonogenic survival endpoints of γ -H2AX foci endpoints. However, chromatid gaps and exchanges were negatively correlated with all the clonogenic survival endpoints. The fate of chromatid gaps after cell division is unknown, but based on their structure gaps should be relatively benign as compared with other cytogenetic aberrations. Our results, however, suggest it may be more lethal to cells than chromatid breaks.

The University of Tennessee Health Science Center (UTHSC) has established an RI Phenotypic Database that is currently curated by Drs. Elissa J. Chesler and Robert W. Williams. The database is searchable and contains both published and unpublished data on several RI strain panels including CXB. The CXB database includes measurements of 633 traits. Querying this database for traits that correlate with low dose rate survival yielded several correlations, the most significant of which involves mammary tumorigenesis (Pearson's product-moment = 0.8636, $p = 0.00892$). The trait, reported by Donald Bailey and colleagues in 1978, is mammary tumor incidence at the end of life in mice infected with Murine Mammary Tumor Virus (MuMTV). We suspect that low dose rate clonogenic survival will correlate with radiation-induced mammary tumor incidence in CXB strains because both endpoints are likely associated with diminished DNA DSB repair. The correlation of LDR survival with Bailey's results is somewhat unexpected because MuMTV causes mammary tumors by insertional mutagenesis rather than DNA damage.

We have genotyped the CXB strains for *Prkdc*. Increased numbers of γ -H2AX foci at low dose rate, and low numbers of surviving colonies in the LDR and SF2 assays are associated with *Prkdc*^{BALB} allele. We interpret this to mean that diminished DSB repair activity due to the hypomorphic BALB/c allele leads to persistence of unrepaired DSB that are detected as γ -H2AX foci and impact clonogenic survival. The association between D0 and *Prkdc* genotype is nearly, but not quite significant. Once again, this may be because D0 is a less sensitive indication of DNA repair capacity than SF2. CXB9 is again the outlier in this comparison.

The results we describe here can lead down several research paths. They can be used to begin searches for the genetic polymorphisms in addition to *Prkdc*^{BALB} that underlie the strain differences. For example, evidence for a modifier gene acting on low dose rate survival and γ -H2AX was discussed above, but the gene is unidentified. The results can also be used to determine if traits that can be assayed in cells are correlated with clinically significant endpoints, specifically cancer susceptibility and sensitivity to normal tissue damage from radiotherapy.

The C57BL/6 and BALB/c strains have different susceptibilities to radiation-induced mammary tumorigenesis. This has been partially attributed to a hypomorphic *Prkdc* allele in the BALB/c strain. Compared to C57BL/6, the BALB/c strain has decreased levels of DNA-PKcs protein as measured by

immunoblotting and decreased DNA-PKcs activity as measured by a kinase assay. The BALB/c variant of DNA-PKcs is less effective than the common variant in DNA DSB repair as measured by the FAR assay. It is hypothesized that the diminished DNA DSB repair capacity of BALB/c variant of DNA-PKcs leads to genomic instability in irradiated mammary epithelial cells which in turn leads to mammary cancer. The link between *Prkdc*^{BALB} and genomic instability has been established, but the link between *Prkdc*^{BALB} and radiation-induced mammary cancer, while likely, remains unproven. Phenotyping the CXB RI strains for incidence of radiation-induced mammary tumors has the potential to establish this link.

Reference

A. Celeste, S. D., M.J. Difilippantonio, O. Fernandez-Capetillo, D.R. Pilch, O.A. Sedelnikova, M. Eckhaus, T. Ried, W.M. Bonner, A. Nussenzweig, (2003). "H2AX haploinsufficiency modifies genomic stability and tumor susceptibility." *Cell* 114: 371-383.

A. Celeste, S. P., P.J. Romanienko, O. Fernandez-Capetillo, H.T. Chen, O.A. Sedelnikova, B. Reina-San-Martin, V. Coppola, E. Meffre, M.J. Difilippantonio, C. Redon, D.R. Pilch, A. Olaru, M. Eckhaus, R.D. Camerini-Otero, L. Tessarollo, F. Livak, K. Manova, W.M. Bonner, M.C. Nussenzweig, A. Nussenzweig, (2002). "Genomic instability in mice lacking histone H2AX." *Science* 296: 922-927.

B. Reina-San-Martin, S. D., L. Hanitsch, R.F. Masilamani, A. Nussenzweig, M.C. Nussenzweig, (2003). "H2AX is required for recombination between immunoglobulin switch regions but not for intra-switch region recombination or somatic hypermutation." *J. Exp. Med* 197: 1767-1778.

B. Wang, S. M., P.B. Carpenter, S.J. Elledge, (2002). "53BP1, a mediator of the DNA damage checkpoint." *Science* 298: 1435-1438.

Bailey, D. (1971). "Recombinant-inbred strains. An aid to finding identity, linkage, and function of histocompatibility and other genes." *Transplantation* 11(3): 325-7.

Bakkenist, C. J., Kastan, M.B. 2003. . 421: 499. (2003). "DNA damage activates ATM through intermolecular autophosphorylation and dimer dissociation." *Nature* 421: 499-501.

Barlow, C., Liyanage, M., Moens, P.B., Deng, C.X., Ried, T., Wynshaw-Boris, A. (1997). "Partial rescue of the prophase I defects of *Atm*-deficient mice by p53 and p21 null alleles." *Nature Genet* 17: 462-466.

Bartek, J., Falck, J., Lukas, J. (2001). "CHK2 kinase—a busy messenger." *Nature Reviews, Mol. Cell Biol.*, 2: 877-886.

Bosotti, R., Isacchi, A., Sonnhammer, E.L. (2000). "FAT: A novel domain in PIK-related kinases." *Trends Biochem. Sci* 25: 225-229.

Byrd, P. J., McConville, C.M., Cooper, P., Parkhill, J., Stankovic, T., McGuire, G.M., Thick, J.A., Taylor, A.M.R. (1996). "Mutations revealed by sequencing the 59 half of the gene for ataxia-telangiectasia." *Hum. Mol. Genet* 5: 145-149.

C.H. Bassing, H. S., D.O. Ferguson, K.F. Chua, J. Manis, M. Eckersdorff, M. Gleason, R. Bronson, C. Lee, F.W. Alt, , *Cell* 114 (2003) 359–370. (2003). "Histone

H2AX. A dosage-dependent suppressor of oncogenic translocations and tumors." *Cell* 114: 359-370.

C.H. Bassing, K. F. C., J. Sekiguchi, H. Suh, S.R. Whitlow, J.C. Fleming, B.C. Monroe, D.N. Ciccone, C. Yan, K. Vlasakova, D.M. Livingston, D.O. Ferguson, R. Scully, F.W. Alt, (2002). "Increased ionizing radiation sensitivity and genomic instability in the absence of histone H2AX." *Proc. Natl. Acad. Sci. U.S.A.* 99: 8173-8178.

Chehab, N. H., Malikzay, A., Appel, M., Halazonetis, T. D. (2000). "Chk2/hCds1 functions as a DNA damage checkpoint in G(1) by stabilizing p53." *Genes Dev* 14: 278-288.

Chen, J. J., Silver, D.P., Walpita, D., Cantor, S.B., Gazdar, A.F., Tomlinson, G., Couch, F.J., Weber, B.L., Ashley, T., Livingston, D.M. Scully, R. (1998). "Stable interaction between the products of the BRCA1 and BRCA2 tumor suppressor genes in mitotic and meiotic cells." *Mol. Cell*, 2: 317-328.

Cromie, G. A., Connelley, J.C., Leach, D.R.F. (2001). "Recombination at double-strand breaks and DNA ends: conserved mechanisms from phage to humans. " *Mol. Cell* 8: 1163-1174.

Davies, A. A., Masson, J.Y., McLlwraith, M.J., Stasiak, A.Z., Stasiak, A., Venkitaraman, A.R., West, S.C. (2001). "Role of BRCA2 in control of the RAD51 recombination and DNA repair protein." *Mol. Cell* 7: 273-282.

Downs, J. A., Lowndes, N.F., Jackson, S.P. (2000) , 408, 1001–1004. (2000). "A role for *Saccharomyces cerevisiae* histone H2A in DNA repair." *Nature* 408: 1001-1004.

Dynan, W. S., Yoo. S. (1998). "Interaction of Ku protein and DNA-dependent protein kinase catalytic subunit with nucleic acids." *Nucleic Acids Res* 26: 1551-1559.

E.P. Rogakou, D. R. P., A.H. Orr, V.S. Ivanova, W.M. Bonner, (1998). "DNA double-stranded breaks induce histone H2AX phosphorylation on serine 139." *J. Biol. Chem* 273: 5858–5868.

Elson, A., Wang, Y., Daugherty, C.J., Morton, C.C., Zhou, F., Campos-Torres, J. and Leder, P. (1996) , 93, 13084–13089. (1996). "Pleiotropic defects in ataxia-telangiectasia protein-deficient mice." *Proc. Natl Acad. Sci. USA* 93: 13084-13089.

Essers, J., van Steeg, H., de Wit, J., Swagemakers, S.M.A., Vermeij, M., Hoeijmakers, J.H.J., Kanaar, R. (2000). "Homologous and non-homologous recombination differentially affect DNA damage repair in mice." *EMBO J* 19: 1703-1710.

Ferguson, D. O., Alt, F.W. (2001). "DNA double strand break repair and chromosomal translocation: lessons from animal models." *Oncogene* 20: 5572-5579.

Friedberg, E. C., Walker, G.C. and Siede W. (1995). "DNA Repair and Mutagenesis." ASM Press, Washington, DC. .

G.S. Stewart, B. W., C.R. Bignell, A.M. Taylor, S.J. Elledge, (2003). "MDC1 is a mediator of the mammalian DNA damage checkpoint." *Nature* 421: 961-966.

Gatei, M., Young, D., Cerosaletti, K.M., Desai-Mehta, A., Spring, K., Kozlov, S., Lavin, M.F., Gatti, R.A., Concannon, P., Khanna, K. (2000). "ATM-dependent phosphorylation of nibrin in response to radiation exposure." *Nature Genet* 25: 115-119.

Gatti, R. A., Berkel, I., Boder, E., Braedt, G., Charmley, P., Concannon, P., Ersoy, F., Foroud, T., Jaspers, N.G., Lange, K., Lathrop, G.M., Leppert, M., Nakamura, Y., O'Connell, P., Patterson, M., Salser, W., Sanal, O., Silver, J., Sparkes, R.S., Susi, E., Weeks, D.E., Wei, S., White, R., Yoder, F. (1988). "Localization of an ataxia telangiectasia gene to chromosome 11q22-23." *Nature* 336: 577-580.

Giaccia, A. J., Kastan, M. B. (1998). "The complexity of p53 modulation: emerging patterns from divergent signals. ." *Genes Dev* 12: 2973-2983.

Gilad, S., Khosravi, R., Uziel, T., Ziv, Y., Rotman, G., Savitsky, K., Smith, S., Harnik, R., Shkedi, D., Frydman, M., Chessa, L., Sanal, O., Portnoi, S., Goldwicz, Z., Jaspers, N.G.J., Gatti, R.A., Lenoir, G., Lavin, M.F., Tatsumi, K., Wegner, R.D., Shiloh, Y., Bar-Shira, A. (1996). "Ataxia-telangiectasia: predominance of mutations that inactivate the ATM protein by truncations or large deletions." *Hum. Mol. Genet* 5: 433-439.

Haber, J. E. (2000). "Partners and pathways—repairing a double-strand break." *Trends Genet* 16: 259-264.

Hartley, K., Gell, D., Smith, G.C., Zhang, H., Divecha, N., Connelly, M.A., Admon, A., Lees-Miller, S.P., Anderson, C.W., Jackson, S.P. (1995). *Cell* 82: 849-856.

Haupt, Y., Maya, R., Kazanietz, A., Oren, M. (1997). "Mdm2 promotes the rapid degradation of p53." *Nature* 387: 296-299

Herzog, K. H., Chong, M.J., Kapsetaki, M., Morgan, J.I., McKinnon, P.J. (1998). "Requirement for Atm in ionizing radiation induced cell death in the developing central nervous system." *Science* 280: 1089-1091.

Hirao, A., Kong, Y.Y., Matsuoka, S., Wakeham, A., Ruland, J., Yoshida, H., Liu, D., Elledge, S.J., Mak, T.W. (2000), 287, 1824-1827. (2000). "DNA damage-induced activation of p53 by the checkpoint kinase Chk2. ." *Science* 287: 1824-1827.

- Hoeijmakers, J. H. J. (2001). "genome maintenance mechanisms for preventing cancer." *G. Nature* 411: 366–374.
- I.M. Ward, K. M., K.G. Jorda, J. Chen, , *J. Biol. Chem.* 278 (2003) 19579–19582. (2003). "Accumulation of checkpoint protein 53BP1 at DNA breaks involves its binding to phosphorylated histone H2AX." *J. Biol. Chem* 278: 19579–19582.
- Ivanova, V., Zimonjic, D., Popescu, N., Bonner, WM. . 1994 Sep;94(3):303-6 (1994). "Chromosomal localization of the human histone H2A.X gene to 11q23.2-q23.3 by fluorescence in situ hybridization." *Hum Genet.* 94(3): 303-306.
- J. Kobayashi, H. T., S. Sakamoto, A. Nakamura, K. Morishima, S. Matsuura, T. Kobayashi, K. Tamai, K. Tanimoto, K. Komatsu, (2002). "NBS1 localizes to gamma-H2AX foci through interaction with the FHA/BRCT domain." *Curr. Biol.* 12: 1846–1851.
- Jacks, T., Remington, L., Williams, B.O., Schmitt, E.M., Halachmi, S., Bronson, R.T., Weinberg, R.A. (1994). "Tumor spectrum analysis in p53-mutant mice." *Curr. Biol* 4: 1-7.
- Jackson, S. (2002). "Sensing and repairing DNA double-strand breaks." *Carcinogenesis* 23(5): 687-696.
- Jeggo, P., Taccioli, GE., Jackson, SP. (1995). "Menage à trois: Double strand break repair, V(D)J recombination and DNA-PK " *BioEssays* 17: 949-957.
- Johnson, R. D., Liu,N., Jasin,M. (1999). "Mammalian XRCC2 promotes the repair of DNA double-strand breaks by homologous recombination." *Nature* 401: 397-399.
- Johnson, R. D., Jasin,M. (2000). " Sister chromatid gene conversion is a prominent double-strand break repair pathway in mammalian cells." *EMBO J* 19: 3398-3407.
- K.J. Weber, M. F., , I 64 (1993) 169–178. (1993). "Lethality of heavy ion-induced DNA double-strand breaks in mammalian cells." *nt. J. Radiat. Biol.* 64: 169-178.
- Kato TA, N. H., Weil MM, Genik PC, Little JB, Bedford JS. (2006). "gamma-H2AX foci after low-dose-rate irradiation reveal atm haploinsufficiency in mice." *Radiat Res* 166(1): 47-54.
- Khanna, K. K., Jackson,S.P. (2001). "DNA double-strand breaks: signaling, repair and the cancer connection. ." *Nature Genet* 27: 247-254.
- Khosravi, R. (1999). "Rapid ATM-dependent phosphorylation of MDM2 precedes p53 accumulation in response to DNA damage." *Proc. Natl Acad. Sci. USA* 96: 14973–14977.

- Kim, S. T., Lim, D. S., Canman, C. E., Kastan, M. B. (1999). "Substrate specificities and identification of putative substrates of ATM kinase family members." *J. Biol. Chem* 274: 37538–37543.
- Kitagawa, R., Kastan, M. B. (2005). The ATM-dependent DNA Damage Signaling Pathway.
- Kubbutat, M. H., Jones, S. N., Vousden, K. H. (1997). "Regulation of p53 stability by Mdm2." *Nature* 387: 299-303.
- Lakin, N. D., Jackson, S.P., (1999) 7644–7655. (1999). "Regulation of p53 in response to DNA damage." *Oncogene* 18: 7644-7655.
- Lees-Miller, S. P., Meek, K. (2003). "Repair of DNA double-strand breaks by non-homologous end-joining." *Biochimie* 85: 1161-1173.
- Lengauer, C., Kinzler, K.W. and Vogelstein, B. (1998). "Genetic instabilities in human cancers." *Nature* 396: 643-649.
- Lewis, J. D., D.W. Abbott, J. Ausio, (2003). "A haploid affair: core histone transitions during spermatogenesis." *Biochem. Cell Biol* 81: 131-140.
- Lim, D., Hasty, P.A. (1996). "A mutation in mouse rad51 results in an early embryonic lethal phenotype that is suppressed by a mutation in p53." *Mol. Cell. Biol.* 16: 7133-7143.
- Lim, D. S., Kim, S.T., Xu, B., Maser, R.S., Lin, J.Y., Petrini, J.H.J., Kastan, M.B. (2000). "ATM phosphorylates p95/nbs1 in an S-phase checkpoint pathway." *Nature* 404: 613-617.
- Liu, N., Lamerdin, J.E., Tebbs, R.S. (1998). "XRCC2 and XRCC3, new human Rad51 family members, promote chromosome stability and protect against DNA cross-links and other damages. ." *Mol. Cell* 1: 783-793.
- Luger, K. (2003). "Structure and dynamic behavior of nucleosomes." *Curr. Opin. Genet. Dev* 13: 127-135.
- Matsuoka, S., Huang, M., Elledge, S. J. (1998). "Linkage of ATM to cell cycle regulation by the Chk2 protein kinase." *Science* 282: 1893-1897.
- Maya, R. (2001). "ATM-dependent phosphorylation of Mdm2 on serine 394: role in p53 activation by DNA damage." *Genes Dev.*

Morrison, C., Sonoda, E., Takao, N., Shinohara, A., Yamamoto, K., Takeda, S. (2000). "The controlling role of ATM in homologous recombinational repair of DNA damage." *EMBO J* 19: 463-471.

O. Fernandez-Capetillo, H. T. C., A. Celeste, I. Ward, P.J. Romanienko, J.C. Morales, K. Naka, Z. Xia, R.D. Camerini-Otero, N. Motoyama, P.B. Carpenter, W.M. Bonner, J. Chen, A. Nussenzweig, (2002). "DNA damage-induced G2-M checkpoint activation by histone H2AX and 53BP1." *Nat. Cell Biol* 4: 993-997.

O. Fernandez-Capetillo, S. K. M., A. Celeste, P.J. Romanienko, R.D. Camerini-Otero, W.M. Bonner, K. Manova, P. Burgoyne, A. Nussenzweig, (2003). "H2AX is required for chromatin remodeling and inactivation of sex chromosomes in male mouse meiosis." *Dev. Cell* 4: 497-508.

Okayasu R, S. K., Yu Y, Silver A, Bedford JS, Cox R, Ullrich RL. (2000). "A deficiency in DNA repair and DNA-PKcs expression in the radiosensitive BALB/c mouse." *Cancer Res* 60(16): 4342-5.

Olive, P. L., Johnston, P.J. (1997). "DNA damage from oxidants: influence of lesion complexity and chromatin organization." *Oncol. Res* 9: 287-294.

Petukhova, G., Stratton, S. and Sung, P. (1998). "Catalysis of homologous DNA pairing by yeast Rad51 and Rad54 proteins." *Nature* 393: 91-94.

Pierce, A. J., Johnson, R.D., Thompson, L.H., Jasin, M. (1999). "XRCC3 promotes homology-directed repair of DNA damage in mammalian cells." *Genes Dev* 13: 2633-2638.

R.A. DiTullio Jr., T. A. M., M. Venere, J. Bartkova, M. Sehested, J. Bartek, T.D. Halazonetis, (2002). "53BP1 functions in an ATM-dependent checkpoint pathway that is constitutively activated in human cancer." *Nat. Cell Biol.* 4: 998-1002.

Rich, T., Allen, R.L. and Wyllie, A.H. (2000). "Defying death after DNA damage." *Nature* 407: 777-783.

Rogakou, E. P., Pilch, D.R., Orr, A.H., Ivanova, V.S., Bonner, W.M. (1998). "DNA double-stranded breaks induce histone H2AX phosphorylation on serine 139." *J. Biol. Chem* 273: 5858-5868.

Rogakou, E. P., Boon, C., Redon, C., Bonner, W.M. (1999). "Megabase chromatin domains involved in DNA double-strand breaks in vivo." *J. Cell Biol* 146: 905-915.

Rotman, G., Shiloh, Y. (1998). "ATM: from gene to function." *Hum Mol Genet* 7(10): 1555-1563.

S. Petersen, R. C., B. Reina-San-Martin, H.T. Chen, M.J. Difilippantonio, P.C. Wilson, L. Hanitsch, A. Celeste, M. Muramatsu, D.R. Pilch, C. Redon, T. Ried, W.M. Bonner, T. Honjo, M.C. Nussenzweig, A. Nussenzweig, (2001). "AID is required to initiate Nbs1/gamma-H2AX focus formation and mutations at sites of class switching." *Nature* 414: 660-665.

Sharan, S. K., Morimatsu, M., Albrecht, U., Lim, D.S., Regel, E., Dinh, C., Sands, A., Eichele, G., Hasty, P., Bradley, A. (1997). "Embryonic lethality and radiation hypersensitivity mediated by Rad51 in mice lacking Brca2." *Nature* 386: 804-810.

Shieh, S. Y., Ahn, J., Tamai, K., Taya, Y., Prives, C. (2000). "The human homologs of checkpoint kinases Chk1 and Cds1 (Chk2) phosphorylate p53 at multiple DNA damage-inducible sites." *Genes Dev* 14: 289-300.

Shiloh, Y. (2003). "ATM and related protein kinases: safeguarding genome integrity." *Nat Rev Cancer* 3: 155-68.

Smith, G., Jackson, S.P. (1999) . 13: 916-934. (1999). "The DNA-dependent protein kinase." *Genes Dev* 13: 916-934.

Sonoda, E., Sasaki, M.S., Buerstedde, J.M., Bezzubova, O., Shinohara, A., Ogawa, H., Takata, M., Yamaguchi Iwai, Y., Takeda, S. (1998). "Rad51-deficient vertebrate cells accumulate chromosomal breaks prior to cell death. ." *EMBO J* 17: 598-608.

T. Stiff, M. O. D., N. Rief, K. Iwabuchi, M. Lobrich, P.A. Jeggo, (2004). "ATM and DNA-PK function redundantly to phosphorylate H2AX after exposure to ionizing radiation." *Cancer Res* 64: 2390-2396.

T.T. Paull, E. P. R., V. Yamazaki, C.U. Kirchgessner, M. Gellert, W.M. Bonner, (2000). "A critical role for histone H2AX in recruitment of repair factors to nuclear foci after DNA damage." *Curr. Biol* 10: 886-895.

Takata, M., Sasaki, M.S., Sonoda, E., Morrison, C., Hashimoto, M., Utsumi, H., Yamaguchi-Iwai, Y., Shinohara, A., Takeda, S. (1998). "Homologous recombination and non-homologous end-joining pathways of DNA double-strand break repair have overlapping roles in the maintenance of chromosomal integrity in vertebrate cells." *EMBO J* 17: 5497-5508.

Takata, M., Sasaki, M.S., Tachiiri, S., Fukushima, T., Sonoda, E., Schild, D., Thompson, L.H., Takeda, S. (2001). "Chromosome instability and defective recombinational repair in knockout mutants of the five Rad51 paralogs." *Mol. Cell. Biol.* 21: 2858-2866.

Taylor, B. (1978). "Recombinant inbred strains: Use in gene mapping. In: Morse III HC (ed), *Origins of Inbred Mice.* ." Academic Press: 423-438.

- Tsuzuki, T., Fujii, Y., Sakumi, K., Tominaga, Y., Nakao, K., Sekiguchi, M., Matsushiro, A., Yoshimura, Y., Morita, T. (1996). "Targeted disruption of the Rad51 gene leads to lethality in embryonic mice." *Proc. Natl Acad. Sci. USA* 93: 6236-6240.
- Uziel, T., Savitsky, K., Platzer, M., Ziv, Y., Helbitz, T., Nehls, M., Boehm, T., Rosenthal, A., Shiloh, Y., Rotman, G. (1996). "Genomic organization of the ATM gene." *Genomics* 33: 317-320.
- Van Dyck, E., Stasiak, A.Z., Stasiak, A., West, S.C. (1999). "Binding of double-strand breaks in DNA by human Rad52 protein." *Nature* 398: 728-731.
- Walker, J. R., Corpina, R.A., Goldberg, J. (2001). "Structure of the Ku heterodimer bound to DNA and its implications for double-strand break repair." *Nature* 412: 607-614.
- Westphal, C. H., Rowan, S., Schmaltz, C., Elson, A., Fisher, D.E., Leder, P. (1997). "atm and p53 cooperate in apoptosis and suppression of tumorigenesis, but not in resistance to acute radiation toxicity." *Nature Genet* 16: 397-401.
- Weterings, E., Gend, DC. (2004). "The mechanism of non-homologous end-joining: a synopsis of synapsis." *DNA Repair* 3: 1425-1435.
- Wood, R. D., Mitchell, M., Sgouros, J., Lindahl, T. (2001). "Human DNA repair genes." *Science* 291(1284-1289).
- Wu, R. S., Panusz, H.T., Hatch, C.L., Bonner, W.M. (1986). "Histones and their modifications." *CRC Crit. Rev. Biochem* 20: 201-263.
- Wu, X., 477-482 (2000). (2000). "ATM phosphorylation of Nijmegen breakage syndrome protein is required in a DNA damage response." *Nature* 405: 477-482.
- X. Xu, D. F. S. (2003). "NFBD1/MDC1 regulates ionizing radiation-induced focus formation by DNA checkpoint signaling and repair factors." *FASEB J* 17: 1842-1848.
- Xu, Y., Baltimore, D. (1996). "Dual roles of ATM in the cellular response to radiation and in cell growth control." *Genes Dev* 10: 2401-2410.
- Xu, Y., Ashley, T., Brainerd, E.E., Bronson, R.T., Meyn, S.M., Baltimore, D. (1996). "Targeted disruption of ATM leads to growth retardation, chromosomal fragmentation during meiosis, immune defects and thymic lymphoma." *Genes Dev* 10: 2411-2422.
- Yongjia Yu, R. O., Michael M. Weil, Andy Silver, Maureen McCarthy, Ryan Zabriskie, Scott Long, Roger Cox, and Robert L. Ullrich (2001). "Elevated Breast Cancer Risk in Irradiated BALB/c Mice Associates with Unique Functional

Polymorphism of the Prkdc (DNA-dependent Protein Kinase Catalytic Subunit) Gene." *CANCER RESEARCH* 61: 1820-1824.

Zhao, S., Weng, Y.C., Yuan, S.S.F. (2000). "Functional link between ataxia-telangiectasia and Nijmegen breakage syndrome gene products." *Nature* 405: 473-477.

Zhou, B. B. (2000). "Caffeine abolishes the mammalian G(2)/M DNA damage checkpoint by inhibiting ataxiatelangiectasia- mutated kinase activity." *J. Biol. Chem* 275: 10342-10348.

Zhou, B. B., Elledge, S.J. (2000). "The DNA damage response: putting checkpoints in perspective." *Nature* 408: 433-439.